~~New~~Monthly new water fractions and their relationships to climate and catchment properties across Alpine rivers

Marius G. Floriancic[1,2], Michael P. Stockinger[3], James W. Kirchner[1,4], Christine Stumpp[3]

[1] Dept. of Environmental Systems Science, ETH Zürich, Zürich, Switzerland

[2] Dept. of Civil, Environmental and Geomatic Engineering ETH Zürich, Zürich, Switzerland

[3] Department of Water, Atmosphere and Environment, Institute of Soil Physics and Rural Water Management, University of Natural Resources and Life Sciences, Muthgasse 18, 1190 Vienna, Austria

[4] Swiss Federal Research Institute WSL, Birmensdorf, Switzerland

Correspondence to: Marius G. Floriancic (floriancic@ifu.baug.ethz.ch)

Abstract. The Alps are a key water resource for central Europe, providing water for drinking, agriculture, and hydropower production. Thus, understanding runoff generation processes of Alpine streams is important for sustainable water management. It is currently unclear how much streamflow is derived from old water stored in the subsurface, versus more recent precipitation that reaches the stream via near-surface quick flow processes. It is also unclear how this partitioning varies across different Alpine catchments in response to hydroclimatic forcing and catchment characteristics. Here, we use stable water isotope time series in precipitation and streamflow to quantify the young water fractions F_{yw} (i.e., the fraction of water younger than approximately 2-3 months) and new water fractions F_{new} (here, the fraction of water younger than one month) in streamflow from 32 Alpine catchments. We contrast these measures of water age between summer and winter and between wet and dry periods, and correlate them with hydroclimatic variables and physical catchment properties.

New water fractions F_{new} varied from 9.~~6~~2 % in rainfall-dominated catchments, to 9.6 % in hybrid catchments, to 3.5 % in snow-dominated catchments (mean across all catchments = 7.1 %). Young water fractions F_{yw} were approximately twice as large (reflecting their longer time scale), varying from 17.6 % in rainfall-dominated catchments to 16.6 % in hybrid catchments, to 10.1 % in snow-dominated catchments (mean across all catchments = 14.3 %). New water fractions were negatively correlated with catchment size (Spearman rank correlation r_S = -0.38), q_{95} baseflow (r_S = -0.36), catchment elevation (r_S = -0.37), total catchment relief (r_S = -0.59), and the fraction of slopes steeper 40° (r_S = -0.48). Large new water fractions, implying faster transmission of precipitation to streamflow, are more prevalent in small catchments, at low elevations, with small elevation ~~gradients~~differences, and with large forest cover (r_S = 0.36). New water fractions averaged 3.3 % following dry antecedent conditions, compared to 9.3 % after wet antecedent conditions. Our results quantify how hydroclimatic and physical drivers shape the partitioning of old and new waters across the Alps, thus indicating which

landscapes transmit recent precipitation more readily to streamflow, and which landscapes tend to retain water over longer periods. Our results further illustrate how new water fractions may find relationships that remained invisible with young water fractions.

1.   1 Introduction

The Alps are often referred to as the "water tower of Europe", as they contribute disproportionally high fractions of streamflow of European rivers (Weingartner et al., 2007). They provide water for agriculture, domestic use, and hydropower production, not only in the Alpine region, but also for approximately 170 million people living in the downstream basins (Mastrotheodoros *et al.*, 2020). Thus, it is important to understand the origins of streamflow in Alpine rivers and how they might change in future climates (Briffa et al., 2009). So far, little is known about the transport and storage of the waters that become Alpine river flow, i.e., to what extent streamflow originates from old water stored in the subsurface, and to what extent streamflow consist of more recent precipitation reaching the stream via near-surface quick flow processes. Across the Alps, contributions from both slow subsurface flow and fast surface or near-surface flow processes are poorly understood (Hayashi, 2019). It is likewise unclear how these slow and fast flow processes, and thus the partitioning of old and new water in Alpine streams, are related to hydroclimatic forcing and physical catchment characteristics across different Alpine catchments.

Stable water isotopes are essential tools for estimating the contribution of different sources to streamflow and for assessing how this source partitioning varies with precipitation characteristics and catchment wetness conditions (Segura et al., 2012). Stable water isotopes have been measured in many catchments worldwide, and data compilations are available for the globe, e.g., the Global Network of Isotopes in Rivers GNIR (~~IAEA, 2019a~~IAEA; 2022) and the Global Network of Isotopes in Precipitation GNIP (~~IAEA, 2019b), and for some regions and countries, e.g.~~IAEA; 2022), and for some regions and countries, e.g. for Switzerland (Staudinger *et al.*, 2020), as well as for individual intensively studied catchments (e.g., Hubbard Brook, Plynlimon, Alptal). Although most multi-catchment time series have been sampled at low temporal frequency, they can nonetheless be used to assess the mixture of streamflow sources on time scales similar to their sampling intervals. They can thus yield insights into how long it takes until precipitation becomes streamflow or, in turn, how much streamflow is coming from recent precipitation versus from water that has been stored in the catchment over longer time scales (Hrachowitz et al., 2009).

Many previous studies assessed the fraction of "event" water by hydrograph separation using two-component mixing models (Klaus and McDonnell, 2013). Prior to the widespread use of stable water isotopes and other conservative tracers, it was assumed that stormflow mostly originated from recent rainfall that travelled rapidly to the stream via overland flow or preferential subsurface flowpaths (Kirchner et al., 2023). This conceptual model was overthrown by tracer studies that

showed that although stream discharge responds quickly to rainfall inputs, recent precipitation makes up only a small fraction of stormflow (Sklash and Farvolden, 1979; Neal and Rosier, 1990; McDonnell and Beven, 2014), a phenomenon often referred to as the "old water paradox" (Kirchner, 2003; McDonnell *et al.*, 2010). Instead of flowing rapidly to the stream, most precipitation instead infiltrates and mobilizes older water from subsurface storage (von Freyberg *et al.*, 2017; von Freyberg *et al.*, 2018). Thus, subsurface storage supplies a large fraction of streamflow, not only during baseflow conditions but also during high flow events (Browne, 1981; Fleckenstein *et al.*, 2006; Floriancic *et al.*, 2022).

Although aquifer waters can be very old (Gleeson *et al.*, 2016; Jasechko *et al.*, 2017), streamwaters derived from them are typically much younger (Berghuijs and Kirchner, 2017). The explanation for this apparent paradox is that hydraulic conductivities in aquifers vary by orders of magnitude (Gleeson et al., 2011b), with the faster flowpaths transmitting disproportionally more water, which, because it flows faster, is younger than the waters left behind in the slower flowpaths (Berghuijs and Kirchner, 2017; Kirchner *et al.*, 2023). In global-scale syntheses, Jasechko *et al.* (2016, 2017) found that although most groundwaters are dominated by fossil waters, 25% of global streamflow is younger than 1.5 - 3 months. According to Jasechko *et al.* (2016), rivers draining mountainous regions tend to have smaller fractions of young water than rivers draining flatter terrain. Jasechko *et al.* (2016) explain this finding by arguing that steeper areas allow for deeper vertical infiltration and thus a greater predominance of deeper, slower flowpaths. However, it remains unclear whether the association between steep terrain and young water fractions is consistent across the European Alps and to what extent these results are influenced by other hydroclimatic variables and physical catchment properties.

Recent studies assessed the impact of catchment properties on the fraction of young water, defined as the fraction of streamflow that is younger than approximately 2-3 months, which can be inferred from the amplitude of seasonal tracer cycles in precipitation and streamflow (Kirchner 2016a; 2016b). For example, von Freyberg *et al.* (2018) found that young water fractions tend to be smaller in steeper terrain, and Ceperley *et al.* (2020) found a decrease in young water fractions above an elevation of 1500 m asl. across Swiss & Italian Alpine catchments. Von Freyberg et al. (2018) also found that higher fractions of young water were associated with higher antecedent catchment wetness, as well as with hydro-climatic factors and catchment characteristics that favor faster transmission of waters to the stream (wet climates, low subsurface permeability, high drainage density). Stockinger *et al.* (2019) found that young water fractions were not related to climate but inversely related to the ratio of average discharge to average precipitation. Catchment area has previously been identified as a major control on catchment mean transit time (DeWalle *et al.*, 1995; Soulsby *et al.*, 2000), but has not been found to be significantly related to young water fractions (von Freyberg *et al.,* 2018).

Gentile *et al.* (2023) have argued that young water fractions should depend on the fraction of catchment area covered by unconsolidated debris deposits and the fraction of baseflow, and von Freyberg *et al.* (2018) found a significant positive correlation between young water fractions and the fraction of the catchment covered by forests. Previous studies of young

water fractions in the Alpine region have primarily focused on small headwater catchments (Gentile *et al.*, 2023; von Freyberg *et al.*, 2018; Ceperley *et al.,* 2020) and did not include larger downstream basins. Whereas young water fractions have been widely used to assess how hydroclimatic and physiographic properties shape catchment transport, new water fractions have thus far remained under-exploited for this purpose. To date, no studies have systematically linked new water fractions to hydroclimatic drivers and physical catchment properties, using datasets that include both headwater catchments and larger downstream basins.

For this study we compiled time series of streamflow, precipitation, stable water isotopes for 32 catchments across the Austrian and Swiss Alps, spanning a wide range of catchment sizes and elevation gradients. We analyzed these time series using two recently developed methods for assessing the relative proportions of younger and older water in streamflow, young water fractions F_{yw} (Kirchner 2016a; 2016b; von Freyberg *et al.*, 2017) and new water fractions F_{new} (Kirchner 2019; Knapp *et al.*, 2019; Kirchner and Knapp 2020), to address the following research questions:

- How much new and young water can be found in Alpine ~~rivers~~catchments of different sizes?

- How do new water fractions vary between different wetness conditions and seasons?

- How do new water fractions vary with antecedent precipitation ~~intensity~~ across Alpine rivers?

- How do new water fractions propagate downstream from headwater catchments to the large basins of the Danube and Rhine catchments?

- Which hydroclimatic variables (climate and streamflow response) and physical catchment properties (topography, lithology, landuse) are associated with larger or smaller fractions of new water?

2.   Methods and Available Data

2.1. Precipitation and Streamflow Data

The analysis is based on 32 Austrian and Swiss Alpine catchments for which streamflow isotope data were available (see Figure 1 and Table 1). Daily discharge time series for 12 of the 20 Swiss sites were obtained from the CH-IRP database (Staudinger *et al.*, 2020). Discharge time series for the remaining 8 Swiss sites and for all 12 Austrian sites were obtained from the Federal Office of the Environment "Hydrological Data and forecasts" database (~~FOEN, 2022a~~FOEN; 2022a) and the "Hydrographisches Jahrbuch" contained in the WISA database (~~Umweltbundesamt, 2022a),~~Umweltbundesamt; 2022a),

130 respectively. Daily catchment averages of precipitation for all 32 sites (12 WISA, 8 FOEN, 12 CH-IRP) were obtained from the gridded precipitation dataset E-OBS (version 20.0e) at 0.1-degree resolution covering the period 1980–2014 (Cornes *et al.*, 2018). For this purpose, the catchment boundaries for all 32 gauging stations were extracted from the Copernicus EU-DEM v1.1 at 25 m resolution using the ArcMap 10.6 Spatial Analyst toolbox.
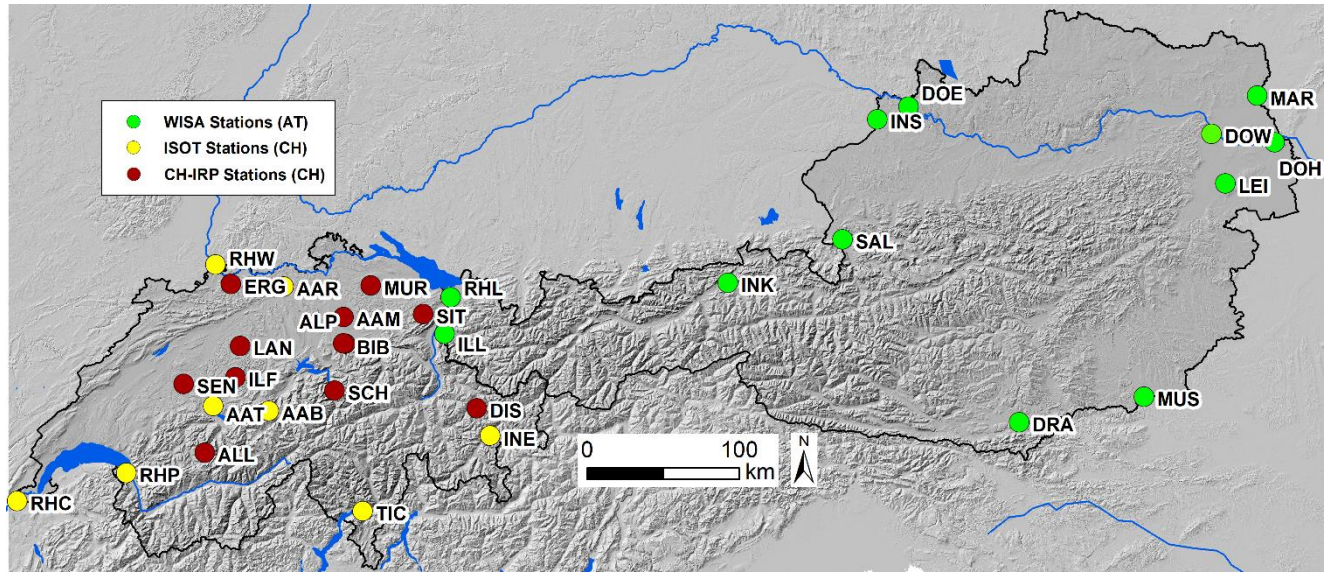
Figure 1: Location of the streamflow isotope sampling sites in Austria (WISA database – green markers) and Switzerland (ISOT database – yellow markers, CH-IRP database – red markers). The hillshade in this map is based on the EU-DEM v1.1. available through funding by the European Union.

140 **2.2. Isotope Data**

We compiled streamflow and precipitation isotope data for 32 catchments across the Austrian and Swiss Alps (see Figure 1 and Table 1). Monthly streamflow isotopes for the 12 Austrian sites were obtained from the WISA "H2O Fachdatenbank" database (Umweltbundesamt, 2022b) and for 8 Swiss stations from the NAQUA ISOT ("Nationalen

145 Grundwasserbeobachtung – Isotopendaten") database (FOEN, 2022b).Umweltbundesamt; 2022b), and for 8 Swiss stations from the NAQUA ISOT ("Nationalen Grundwasserbeobachtung – Isotopendaten") database (FOEN; 2022b; Schürch et al., 2003). Streamflow isotopes for 12 additional stations across the Swiss Alps were obtained from the CH-IRP database (Staudinger *et al.*, 2020). Many of the study catchments lack direct measurements of precipitation isotopes within the catchment boundaries. In all but the largest catchments where direct measurements are available, they are available only at

150 single sampling locations. Because precipitation isotopes vary with altitude and other factors, we did not interpolate

5

individual station measurements across our study catchments, but instead relied on the monthly gridded precipitation isotope reanalysis database Piso.AI (Nelson *et al.*, 2021), which we averaged within the boundaries of each of our study catchments.

Table 1: Data summary for study catchments, including original database ID, site name abbreviation (site code), river and gauge names, database name, latitude and longitude at catchment outlet, and number of samples for δ¹⁸O and δ²H in the publicly available streamflow isotope datasets: WISA (National Austrian Isotope database; n = 12), ISOT (National Swiss isotope database; n = 8) and CH-IRP (Staudinger *et al.*, 2020; n = 12).

org ID	Site code	River	Gauge	Data origin	long (deg.)	lat (deg.)	# ^{18}O	# ^{2}H
IO20000010	DRA	Drau	Neubrücke	WISA	14.46	32.36	162	162
IO30000009	DOH	Donau	Hainburg	WISA	16.48	56.08	174	174
IO30000014	LEI	Leitha	Brodersdorf	WISA	16.47	28.55	175	175
IO30000015	MAR	March	Angern	WISA	16.48	49.25	156	156
IO40000001	DOE	Donau	Engelhartszell	WISA	13.48	43.3	168	168
IO40000012	INS	Inn	Schärding	WISA	13.48	25.26	172	172
IO50000018	SAL	Salzach	Salzburg	WISA	13.47	4.44	172	172
IO60000016	MUS	Mur	Spielfeld	WISA	15.46	37.42	175	175
IO70000013	INK	Inn	Kirchbichl	WISA	12.47	4.3	176	176
IO80000011	ILL	Ill	Gisingen	WISA	9.47	35.13	175	175
IO80000017	RHL	Rhine	Lustenau	WISA	9.47	39.26	174	174
IO90000005	DOW	Donau	Wien-Nußdorf	WISA	16.48	23.13	166	166
NIO08	RHW	Rhine	Weil	ISOT	7.59	47.60	361	195
NIO01	AAB	Aare	Brienzwiler	ISOT	8.09	46.75	347	346
NIO07	AAT	Aare	Thun	ISOT	7.61	46.76	255	254
NIO02	AAR	Aare	Brugg	ISOT	8.19	47.48	319	316
NIO04	RHP	Rhône	Porte du Scex	ISOT	6.89	46.35	329	326
NIO09	RHC	Rhône	Chancy	ISOT	5.97	46.15	102	102
NIO05	TIC	Ticino	Riazzino	ISOT	8.91	46.16	287	285
NIO06	INE	Inn	S-chanf	ISOT	10.00	46.62	226	226
AAM	AAM	Aa	Mönchaltorf	CH_IRP	8.47	47.19	95	95
ALL	ALL	Allenbach	Adelboden	CH_IRP	7.33	46.29	173	173
ALP	ALP	Alp	Einsiedeln	CH_IRP	8.44	47.09	319	319
BIB	BIB	Biber	Biberbrugg	CH_IRP	8.43	47.09	318	318
DIS	DIS	Dischmabach	Davos	CH_IRP	9.52	46.46	128	128
ERG	ERG	Ergolz	Liestal	CH_IRP	7.44	47.29	223	223
ILF	ILF	Ilfis	Langnau	CH_IRP	7.47	46.56	224	224
LAN	LAN	Langeten	Huttwil	CH_IRP	7.49	47.07	197	197
MUR	MUR	Murg	Wängi	CH_IRP	8.57	47.29	128	128
SCH	SCH	Schaechen	Bürglen	CH_IRP	8.39	46.52	181	181
SEN	SEN	Sense	Thörishaus	CH_IRP	7.21	46.53	198	198
SIT	SIT	Sitter	Appenzell	CH_IRP	9.24	47.19	185	185

2.3. Hydroclimatic variables

We assessed the relationship of isotopic signatures to 9 hydroclimatic variables (Table 2) in all 32 catchments. Daily catchment averaged precipitation from the gridded precipitation dataset E-OBS (version 20.0e) at 0.1-degree resolution (Cornes *et al.*, 2018) was used to calculate the mean annual, winter (November through April) and summer (May through October) precipitation for each of the 32 catchments. The catchment boundaries were used to average mean monthly potential evapotranspiration (*PET*) across each catchment from the "Global Aridity Index and Potential Evapotranspiration Climate Database v2" (Trabucco and Zomer, 2019); from these monthly averages, we also calculated annual, winter (November through April) and summer (May through October) *PET*. The discharge fraction ($q\,P^{-1}$) was calculated by dividing the total annual streamflow (in mm) by the total annual precipitation. The discharge that is exceeded 95% of the time (q_{95} – in mm per day) was obtained from the streamflow duration curve by calculating the 5th percentile of all streamflow values. The use of q instead of Q indicates that the values are divided by area to obtain an area-normalized discharge quantile (in mm per day rather than m^3 per second).

2.4. Physical catchment properties

We assessed the relationship between isotopic signatures to 9 physical catchment properties (Table 3) across all 32 study catchments. We calculated the following six topographic properties: total catchment area, mean catchment elevation, elevation difference (calculated from maximum elevation – minimum elevation), mean catchment slope, the fraction of slope below 10°, and the fraction of slope above 40°. To assess the effect of lithology, we calculated the fraction of (potentially karstified) carbonate sedimentary rocks and the fraction of unconsolidated debris deposits for all catchments. Because plants, such as trees, affect the hydrological cycle by increasing water losses through transpiration, we also calculated the fraction of forest cover for each catchment. From the catchment boundaries, the total catchment area was calculated with the "Tabulate Area" – tool of ArcMap 10.6. The mean, minimum, and maximum catchment elevation were calculated from the Copernicus EU-DEM v1.1 at 25 m resolution using the ArcMap 10.6 Zonal Statistics tool. The mean slope, fraction of slope below 10°, and fraction of slope above 40° were also calculated from the Copernicus EU-DEM v1.1. From the 0.5° resolution raster map GLiM ("Global Lithological Map" - Hartmann and Moosdorf, 2012), the fraction of area of potentially karstified carbonate sedimentary rocks (GLiM class SC) and the fraction of area covered with unconsolidated debris deposits (GLiM class SU) were calculated. From the Copernicus CORINE land cover "CLC 2018" the fraction of area covered by forests was calculated, by combining the three CLC classes broad-leaved forest, coniferous forest, and mixed forest. All geodata mentioned above were extracted using the obtained catchment boundaries and the ArcMap 10.6 Zonal Statistics tool.

2.5. Calculations of young water fractions (F_{yw}) and new water fractions (F_{new})

In seasonal climates, summer precipitation is isotopically heavier and winter precipitation is isotopically lighter, resulting in a seasonal cycle of precipitation isotopes. Kirchner (2016a; 2016b) showed that the young water fraction F_{yw} (the fraction of

streamflow that is younger than 2-3 months) can be estimated from the ratio of the seasonal amplitudes of sinusoidal fits to precipitation and streamflow isotope time series. Fits that are robust against outliers can be obtained using iteratively re-weighted least squares (IRLS); an R script for this approach is available in the supplement of von Freyberg *et al.* (2018). We used results for the volume weighed F_{yw}, because estimates of F_{yw} are more reliable when the sinusoidal isotope fits are volume-weighted by the precipitation and streamflow volumes, and when they are derived from longer time series that yield more stable amplitude estimates (Kirchner 2016a; 2016b; von Freyberg *et al.*, 2018; von Freyberg *et al.*, 2017). .

We also calculated new water fractions (F_{new}) using the ensemble hydrograph separation approach outlined in Kirchner (2019). A major advantage of F_{new} over F_{yw} is that the time scale over which water is considered "young" (2-3 months) depends on the shape of the catchment transit time distribution, which will typically be unknown, whereas the time scale over which water is "new" is directly linked to the sampling frequency of the isotope time series. That is, because our isotope data iswere sampled at monthly resolution, F_{new} estimates the fraction of streamwater that originated from precipitation in the one-month period since the previous streamwater sample was collected.

The ensemble hydrograph separation approach is based on correlations between isotopic fluctuations in streamflow and precipitation (and potentially also other endmembers). It estimates the average contribution of precipitation to streamflow through correlations across an ensemble of precipitation and streamflow isotope samples. This makes it insensitive to unknown or unmeasured endmembers, and avoids the spurious results that can arise in traditional hydrograph separation when the "old water" and "new water" isotopic signatures overlap. While traditional hydrograph separation assesses how fractions of new and old water change over successive time steps (e.g., during an individual storm event), ensemble hydrograph separation can quantify the average fractions of new and old water over ensembles of non-successive time steps reflecting different conditions (e.g., antecedent moisture). This is another major advantage of F_{new} over F_{yw}, and a main goal of this study is to calculate new water fractions across all 32 Alpine catchments for the entire dataset and for subsets of the data reflecting different catchment conditions. Here, we report volume-weighted new water fractions of streamflow ($^{Q}F^{*}_{new}$ in the notation of Kirchner (2019)) calculated using the R script provided by Kirchner and Knapp (2020a) and Kirchner and Knapp (2020b). With ensemble hydrograph separation we could calculate the fraction of streamflow that is "new" since the last streamflow sampling, which for our data is the fraction of streamflow younger than one month.

To assess F_{new} for the driest and wettest half of the dataset, we split our data into two subsets based on monthly precipitation totals recorded prior to sampling and calculated F_{new} separately for the 50 % of sampling dates that received more precipitation and the 50 % of sampling dates that received less precipitation. To assess seasonal differences, we also split the data into the winter (November through April) and summer (May through October) halves of the year. For each of these four subsets of data we then, and calculated F_{new} separately for the winter and summer subsets. We also calculated the fraction of new water as a function of incoming precipitation (as described in Section 3.5 of Kirchner 2019; Section 5.4 of Knapp *et al.*,

8

2019). We expect that higher values of F_{new} will often be associated with higher precipitation totals in the month immediately preceding sampling.

~~Previous studies have indicated that the (volume weighted) fractions of new and young water are related to physical~~
~~catchment properties (e.g., to mean catchment elevation). Thus, for all 32 catchments we calculated the following seven~~
~~topographic properties: total catchment area, mean catchment elevation, elevation difference (calculated from maximum~~
~~elevation – minimum elevation), mean catchment slope, the fraction of slope below 10°, and the fraction of slope above 40°.~~
~~To assess the effect of lithology, we calculated the fraction of (potentially karstified) carbonate sedimentary rocks and the~~
~~fraction of unconsolidated debris deposits for all catchments. Because plants, such as trees, affect the hydrological cycle by~~
~~increasing water losses through transpiration, we also calculated the fraction of forest cover for each catchment.~~

2.6. Statistical measures for data analysis

Isotope data are presented in the delta notation in per mil (‰) of [18]O relative to V-SMOW (Vienna Standard Mean Ocean Water) throughout the paper (the respective ^{2}H plots can be found in the supplement). Overall, both $\delta^{18}O$ and δ^2H should yield similar results if non-equilibrium isotope fractionation processes due to evaporation can be neglected (Craig and Gordon, 1965). Some data are presented in boxplots, in which the horizontal line indicates the median, the box represents the interquartile range, and the whiskers extend to 1.5 times the interquartile range from the first and third quartiles (or to the maximum and minimum values). The dots indicate outliers. Spearman rank correlations were calculated to obtain the correlation coefficient r_S and its associated p-value. Differences between groups of samples were tested using Wilcoxon Signed-Rank tests. Results are presented as statistically significant when $p < 0.05$.

3. Results

3.1. Hydroclimatic variables and catchment characteristics

Among the 32 study sites, average annual precipitation ranges from 611 mm to 1741 mm (mean = 1244 mm), winter precipitation ranges from 211 mm to 748 mm (mean = 534 mm) and summer precipitation ranges from 400 mm to 994 mm (mean = 710 mm). Mean annual *PET* ranges from 669 mm to 912 mm (mean = 825 mm), winter *PET* ranges from 193 mm to 269 mm (mean = 240 mm) and summer *PET* ranges from 496 mm to 657 mm (mean = 586 mm). The ratio of average discharge to average precipitation (q P^{-1}) ranges from 0.10 to 0.78 (mean = 0.38); the q_{95} ranges from 0.09 mm day^{-1} to 1.54 mm day^{-1} (mean = 0.83 mm day^{-1}).

Table 2: Averages of major hydro-climatic variables across the 32 Alpine catchments: mean annual precipitation, winter precipitation, summer precipitation, mean annual potential evapotranspiration, winter potential evapotranspiration, summer potential evapotranspiration (all in mm), the ratio of annual streamflow to annual precipitation (%) and the discharge reached or exceeded 95% of the time (in mm day^{-1}).

Site code	mean annual P	winter P	summer P	annual PET	winter PET	summer PET	$q\ P^{-1}$	q_{95}
[-]	mm	mm	mm	mm	mm	mm	%_f	mm day^{-1}
DRA	1368	534	834	769	215	554	0.30	0.97
DOH	995	401	594	816	225	591	0.29	0.80
LEI	887	333	554	912	259	653	0.11	0.19
MAR	611	211	400	891	234	657	0.10	0.09
DOE	1008	409	599	809	223	586	0.28	0.81
INS	1176	466	710	785	224	561	0.40	1.20
SAL	1364	528	836	745	216	529	0.53	1.54
MUS	1213	448	764	799	226	573	0.21	0.59
INK	1094	443	651	746	215	531	0.46	1.07
ILL	1374	572	802	809	245	564	0.59	1.46
RHL	1417	586	831	797	240	557	0.40	1.16
DOW	1003	405	599	812	224	588	0.29	0.80
RHW	1290	569	721	850	246	604	0.34	1.24
AAB	1271	586	685	774	231	543	0.78	1.37
AAT	1201	580	620	822	250	572	0.58	1.19
AAR	1210	564	646	878	254	624	0.35	1.06
RHP	1086	564	523	813	244	569	0.51	1.26
RHC	1179	604	576	875	260	615	0.45	0.97
TIC	1480	585	895	856	268	588	0.44	1.08
INE	974	408	566	689	193	496	0.61	0.60
AAM	1208	487	721	888	244	644	0.27	0.23
ALL	1251	661	590	853	269	584	0.56	1.29
ALP	1625	674	951	859	258	601	0.44	0.61
BIB	1543	637	905	868	260	608	0.36	0.35
DIS	1211	522	690	690	194	497	0.52	0.72
ERG	1286	613	673	872	246	626	0.17	0.11
ILF	1364	621	743	868	258	610	0.32	0.53
LAN	1322	599	723	886	250	637	0.23	0.73
MUR	1167	471	696	858	239	619	0.30	0.37
SCH	1741	748	994	805	247	557	0.46	1.10
SEN	1240	581	659	884	262	622	0.30	0.52
SIT	1651	685	967	831	250	581	0.35	0.54

The catchments range in size from 29 km^2 to 103'946 km^2 (mean = 13'923 km^2, median = 1562 km^2). The mean catchment elevation varies from 379 m a.s.l. to 2472 m a.s.l. (mean = 1310 m a.s.l.), and the elevation difference varies from 403 m to 4454 m (mean = 2477 m). The mean catchment slope ranges from 4.6° to 50.9° (mean = 20.1°), the fraction of catchment

area with slope < 10° ranges from 9.1 % to 93.2 % (mean = 65 %), and the fraction of catchment area with slope > 40° ranges from 0 to 18.5 % (mean = 6.1 %). The fraction of catchment area covered by carbonate sedimentary rocks ranges from 0 to 80.1 % (mean = 27.4 %), the fraction of area covered by unconsolidated rocks ranges from 0 to 56.1 % (mean = 17.5 %). The fraction of catchment area covered by forests ranges from 3.1 % to 60.3 % (mean = 32.9 %).

Table 3: Catchment averages of physical catchment properties across the 32 Alpine catchments: total catchment area, mean catchment elevation, elevation difference (max-min), mean catchment slope, fraction of area with slope < 10°, fraction of area with slope > 40°, fraction of area with potentially karstified carbonate sedimentary rocks, the fraction of area with unconsolidated debris deposits, and the fraction of area covered by forests.

Site code	area	mean elevation	minimum elevation	elevation difference	mean slope	f slope < 10°	f slope > 40°	f karstified	f debris	f forest
[-]	km²	m asl.	m asl.	m	°	%	%	%	%	%
DRA	10398	1389.8	390.8	3336.9	20.8	78.7	5.8	23.0	0.7	52.0
DOH	103946	796.0	137.8	3843.6	10.2	33.6	2.4	25.6	19.2	37.1
LEI	1588	699.1	194.5	1864.7	12.9	54.5	1.2	40.3	0.0	60.3
MAR	25616	379.3	143.3	1051.5	4.6	11.1	0.0	2.1	27.0	30.4
DOE	77107	838.7	280.3	3701.1	9.7	30.4	2.6	24.1	25.7	34.4
INS	24232	1321.7	305.2	3676.2	18.0	63.0	6.2	27.9	17.1	35.9
SAL	3910	1513.8	429.6	3181.3	24.0	87.0	8.5	32.7	0.0	43.3
MUS	9575	1074.2	246.3	2770.5	17.3	71.8	1.8	18.2	0.0	59.1
INK	9304	1941.2	487.2	3494.2	25.2	88.9	10.0	26.9	3.6	30.0
ILL	1282	1608.2	443.5	2773.5	25.1	87.9	10.3	42.2	0.6	36.0
RHL	6500	1736.6	402.0	3150.8	23.4	85.3	8.5	40.8	18.3	29.3
DOW	101803	806.4	151.9	3829.5	10.3	33.7	2.5	25.7	19.6	37.0
RHW	36435	1049.9	234.8	3899.2	14.1	51.7	4.3	28.2	31.4	31.7
AAB	587	2101.3	571.9	3562.1	27.5	88.7	17.5	23.8	7.0	15.5
AAT	2521	1739.9	553.9	3580.0	24.7	84.3	14.0	51.5	15.8	23.4
AAR	11584	1006.7	339.2	3794.8	12.8	47.0	3.9	29.6	35.3	30.0
RHP	5307	2096.7	377.1	4144.2	25.5	87.8	12.2	21.5	17.8	23.5
RHC	10309	1564.9	335.9	4454.2	19.7	68.6	8.5	25.1	22.2	27.8
TIC	1562	1651.7	200.3	3140.0	28.7	91.2	18.5	9.2	12.0	44.1
INE	625	2472.4	1654.2	2327.3	50.9	86.6	8.7	13.2	17.3	11.3
AAM	49	522.3	444.1	402.5	6.1	9.1	0.0	0.0	23.8	15.8
ALL	29	1866.3	1310.0	1390.2	28.8	89.7	8.1	80.1	17.7	19.7
ALP	46	1160.4	857.8	854.7	19.4	70.8	0.7	48.3	30.6	50.4
BIB	32	1009.4	831.1	637.8	14.9	53.1	0.0	0.8	56.1	42.9
DIS	43	2372.1	1679.1	1401.7	28.7	92.7	6.3	0.0	18.6	3.1
ERG	261	588.8	308.0	855.0	15.0	56.0	0.1	78.0	4.9	43.9

ILF	188	1050.1	683.1	1361.8	25.0	78.1	1.1	5.8	7.4	53.8
LAN	60	760.9	603.4	450.4	12.2	31.6	0.0	0.0	21.5	15.1
MUR	77	652.3	470.7	538.6	12.5	36.6	0.0	0.0	37.9	33.3
SCH	108	1738.7	493.9	2618.1	31.1	93.2	16.4	36.0	17.9	21.2
SEN	351	1079.8	558.2	1566.6	18.1	61.3	1.5	31.5	24.3	35.0
SIT	88	1316.9	772.9	1613.1	25.9	77.0	13.4	63.0	7.2	27.8

3.2. Isotopic variation of precipitation and streamflow across Alpine catchments

285

The seasonal variations of isotope ratios in precipitation and streamflow are expected to be related to the size of the catchment (i.e., more damped streamflow isotope ratios in larger catchments) and the mean catchment elevation (i.e., precipitation isotope ratios are lighter at higher elevations). The relationships of precipitation and streamflow $\delta^{18}O$ signatures to catchment area and elevation are shown in Figure 2. Overall, the amplitudes of the seasonal isotope signatures are damped

290   from precipitation to streamflow. While there is only a weak trend between the isotope ratios and catchment area, precipitation and streamflow isotope ratios are lighter in higher-elevation catchments as expected.

The Spearman rank correlation coefficients (r_S) between catchment area and the median $\delta^{18}O$ for precipitation and streamflow were 0.28 and 0.02, respectively (not significant). The range of variation (max-min) of $\delta^{18}O$ was inversely

295   correlated with catchment area; $r_S = -0.71$ ($p = < 0.05$) and -0.45 ($p = < 0.05$) for precipitation and streamflow, respectively. This suggests that the median of $\delta^{18}O$ precipitation and streamflow isotopes only slightly increases with catchment size, whereas precipitation and streamflow isotopes are significantly less variable over time in larger catchments. Median $\delta^{18}O$ decreased with increasing catchment elevation; $r_S = -0.85$ ($p = < 0.05$) and -0.90 ($p = < 0.05$) for precipitation and streamflow, respectively. Similar results were obtained for $\delta^{2}H$; see Supplementary Material (Figure S1).

300
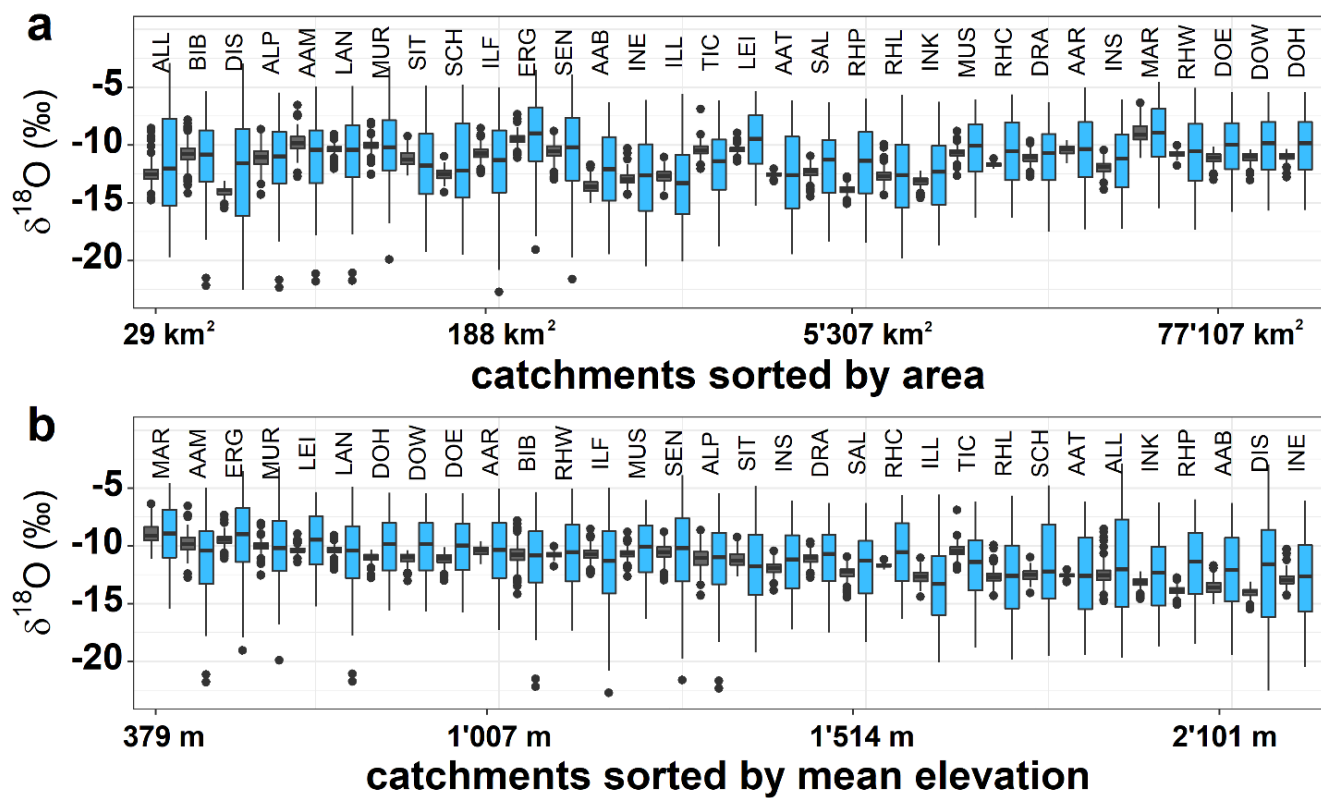
Figure 2: Boxplots of the $\delta^{18}O$ isotopic composition of precipitation (light blue) and streamflow (dark grey) across all 32 Alpine catchments sorted by catchment area from small to large (a) and mean catchment elevation from low to high (b).

3.3. New (F_{new}) and young (F_{yw}) water fractions across Alpine catchments

In Figure 3, the fractions of new water (F_{new}) and young water (F_{yw}) are shown. The catchments are sorted by mean catchment elevation from MAR (March at Angern, 379 m a.s.l.) to INE (Inn at S-canf, 2472 m a.s.l.). Both F_{new} and F_{yw} tended to be smaller at higher mean catchment elevations (r_S = -0.37 and -0.32). However, the study catchments encompass different precipitation and discharge regimes: MAR to BIB are rainfall-dominated (precipitation falls almost exclusively as rain), RHW to DRA are hybrid (both rain and snow can contribute significantly to winter precipitation), and SAL to INE are snow-dominated (most winter precipitation falls as snow). Both F_{new} and F_{yw} differed significantly between rainfall-dominated and snow-dominated catchments as well as between hybrid and snow-dominated catchments ($p < 0.05$). Mean F_{new} varied from 9.2 % in rainfall-dominated catchments and 9.6 % in hybrid catchments to 3.5 % in snow-dominated catchments, and mean F_{yw} varied from 17.6 % in rainfall-dominated, 16.6 % in hybrid catchments to 10.1 % in snow-dominated catchments. F_{new} and F_{yw} were strongly correlated (Pearson R = 0.88), with F_{yw} systematically exceeding F_{new} (Figure 3c). This is expected because F_{yw} expresses the fraction of water younger than 2-3 months, which should always be greater than the fraction of water younger than one month (i.e., F_{new} estimated from monthly data).

320
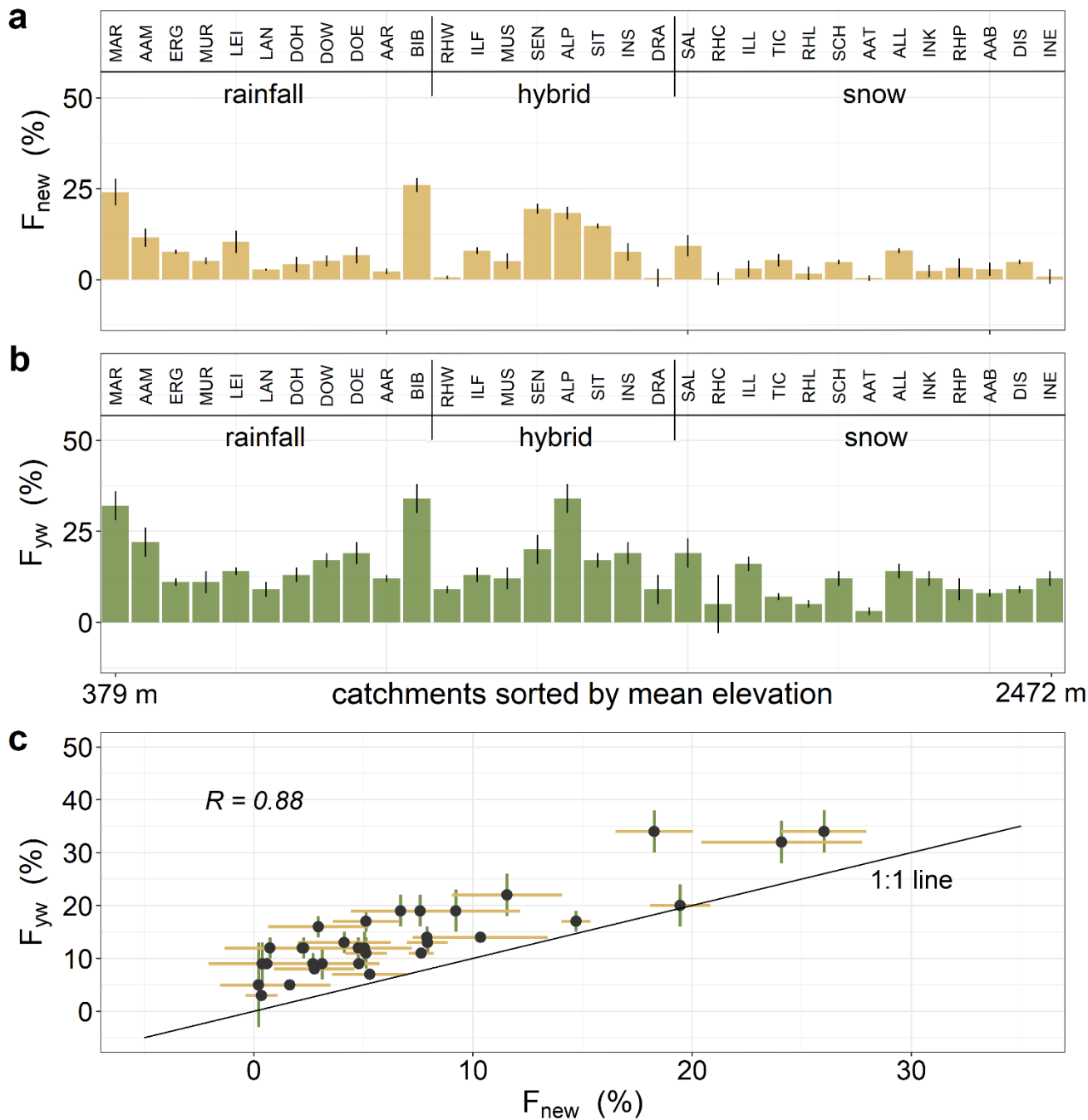
Figure 3: New water fractions (a) and young water fractions (b) for all catchments sorted by elevation. F_{new} and F_{yw} are smaller in catchments of higher mean elevation. F_{new} and F_{yw} are strongly correlated, with F_{yw} being systematically higher as indicated by the points lying above the 1:1 line (c).

325

15

### 3.4. New water fractions (F_{new}) across Alpine catchments for different subsets of data

In the following section, the potential of the F_{new} analysis is further explored, as F_{new} can be calculated for different subsets of the data; for example, for different antecedent conditions or different seasons. For most catchments, F_{new} was larger in the wettest (highest-precipitation) 50% of all months than in the driest half (mean F_{new} = 9.3 % and 3.3 %, respectively; $p <$ 0.05). F_{new} also tended to be larger in summer than in winter (mean F_{new} = 12.7 % and 8.9 %, respectively; $p < 0.05$). This is not surprising, because across most of the Alps, precipitation is typically higher in the summer than the winter (mean across all catchments of our study 710 mm in summer and 534 mm in winter; only RHP and ALL receive more precipitation in winter than in summer). Readers should note that we did not consider the delayed timing of snowmelt explicitly as a delayed precipitation input (as suggested in von Freyberg et al.; 2018) but only consider the timing of precipitation.
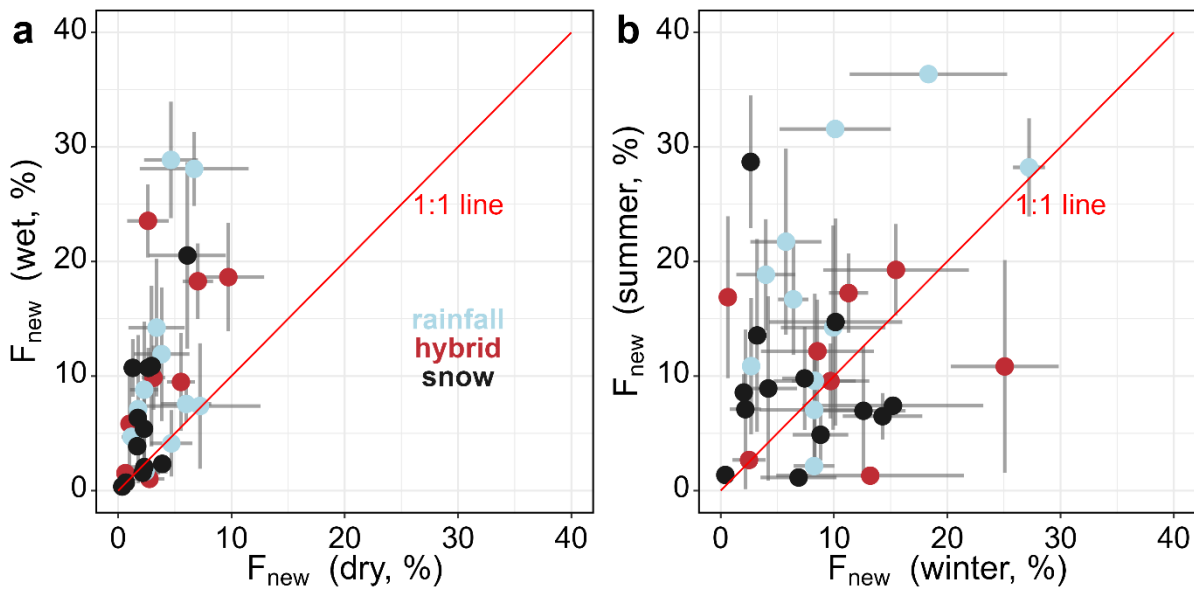
Figure 4: New water fractions for the driest and wettest half of the dataset (a), and for the winter and summer half of the dataset (b). The colours indicate the different precipitation regimes (light blue for rainfall, red for hybrid, and black for snow dominated). New water fractions tend to be higher in wet periods with few exceptions. Summer new water fractions tend to be higher in most catchments.

We also calculated the fraction of new water for different ranges of monthly precipitation. It is expected that F_{new} is larger for months with more incoming precipitation. As shown in Figure 5, 18 of our 32 study catchments show increases in F_{new} above a certain threshold in monthly precipitation rates, i.e. roughly 70 mm for MAR, roughly 110 mm for AAM, 175 mm

for MUS, DOE, DOH, DOW, ERG, MUR, RHL, BIB and LEI, roughly 200 mm for SEN, ~~DOW~~ALP, LAN, INK, SIT and
INS, and roughly 225 mm for SAL. For these catchments, it is evident that - after the threshold precipitation inputs are
reached - the more recent precipitation fell, the more recent precipitation can be found in streamflow, as indicated by
increasing F_{new}. For 14 out of 32 catchments, more incoming precipitation does not raise F_{new} above ~10% (Figure ~~5b~~S2),
suggesting catchment storage is large enough to damp tracer fluctuations, even under high monthly precipitation rates. These
different responses to incoming precipitation are associated with differences in catchment elevation and slope. The eighteen
catchments in which F_{new} increased substantially above a precipitation threshold (Figure 5a) have a mean elevation of 1068
m a.s.l. and a mean slope of 16.1°, whereas the 14 catchments in which F_{new} remained small (Figure ~~5b~~S2) are, on average,
both higher (mean elevation of 1584 m a.s.l.) and steeper (mean slope of 24.3°); both differences are statistically significant
($p < 0.05$).
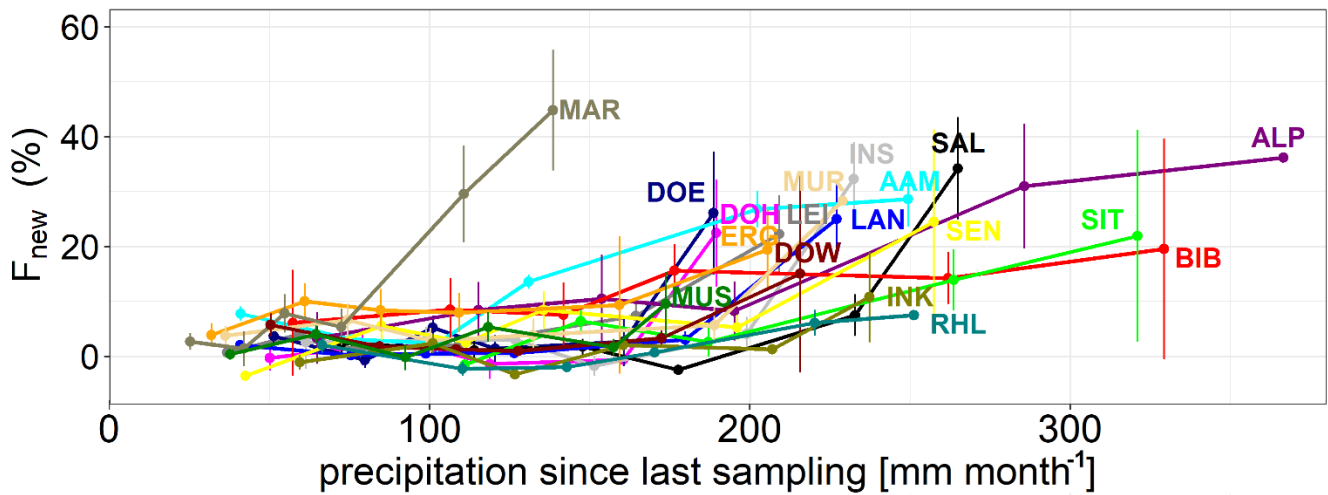
Figure 5: The volume weighted fraction of new water (F_{new}) as a function of monthly precipitation totals during the month immediately preceding the sampling date. 18 out of the 32 catchments, as shown in ~~(a)~~, exhibit a clear increase in F_{new} at higher monthly precipitation totals. In these cases, F_{new} increases at monthly precipitation rates exceeding ~175 mm month⁻¹. For 14 out of 32 catchments, F_{new} remains below 10% even at the highest monthly precipitation totals (~~b~~shown in Figure S2 in the Supplementary Material).

3.5. Downstream propagation of F_{new} in Danube and Rhine

New water fractions F_{new} were mapped across 7 sub-catchments of the Danube river basin (Figure 6 a & c). Two headwater
basins of the Inn have exceptionally small F_{new} values (0.7 % at INE and 2.3% at INK), potentially due to snowpack storage
in these high-elevation catchments. It should also be noted that INE is sampled directly below several large lakes (St. Moritz,

17

Engadin, Switzerland), and thus the damped isotope signal probably reflects mixing and storage within those lakes. The remaining 5 Danube catchments exhibit a weak declining trend in F_{new} with increasing catchment area, which nonetheless results in a perfect rank correlation (r_S=-1.0) due to the small sample size (if all 7 sub-catchments are considered together, the rank correlation is non-significant).

The new water fractions F_{new} were also mapped across the 18 subcatchments of the Rhine river basin (Figure 6 b & d). The smaller headwater catchments tend to have larger F_{new} (i.e., F_{new} exceeds 8% for BIB, ALP, AAM, SIT, and SEN), suggesting that these headwater streams contain relatively large proportions of recent precipitation. These five headwater catchments are at low to intermediate mean elevations (522-1317 m a.s.l.). Across the Rhine basin, smaller catchments tend to have higher F_{new} ($r_S = -0.67$, p<0.05; Figure 6d).
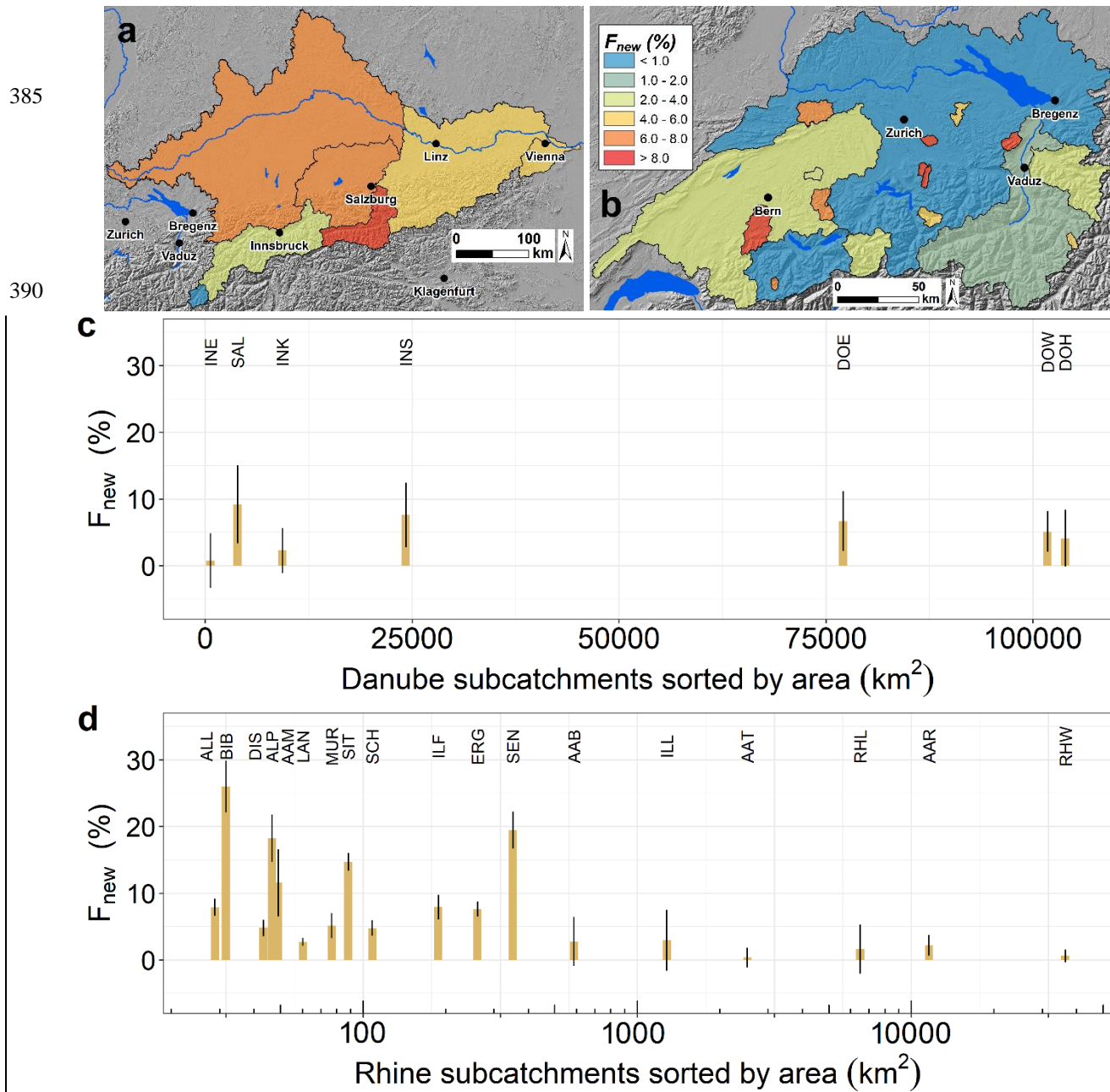
Figure 6: New water fractions (*F_new*) mapped across the subcatchments of the Danube (a) and Rhine (b) basins (n=7 and n=18, respectively), and *F_new* as a function of catchment area for the Danube (c) and Rhine (d) subcatchments. The Inn headwater catchments in the southeast of the Danube basin (INE and INK) have small *F_new*. For the other subcatchments in the Danube and Rhine basins, the expected decrease in *F_new* with increasing catchment size is

evident. Note that the x-axis in subpanel (d) is logarithmic. The hillshades in the maps are based on the EU-DEM v1.1. available through funding by the European Union.

3.6. Relationships between F_{new} and hydroclimatic variables

400

Previous studies indicated that the (volume weighted) fractions of new water are related to hydroclimatic variables, e.g., catchments have larger F_{new} following wet antecedent conditions (Knapp *et al.*, 2019). Thus, we analyzed the relationships between F_{new} and a range of climate variables (annual, summer, and winter precipitation sums, and annual, summer and winter evapotranspiration sums) as well as the ratio of total discharge to total precipitation ($q\,P^{-1}$), and the discharge that is

405   reached or exceeded 95% of the year (q_{95}). As Figure 7 shows, F_{new} values were only weakly related to catchment annual, winter, and summer precipitation. Thus, mean annual or seasonal precipitation is a poor predictor of F_{new}, despite the fact that F_{new} does tend to be higher in wetter months (Figure 4). F_{new} was more strongly correlated to the amount of annual *PET* and summer *PET* ($r_S = 0.41$ and 0.40, respectively). F_{new} was also negatively correlated with the $q\,P^{-1}$ ratio ($r_S = -0.36$, $p <$ 0.05) or, positively correlated with the fraction (P-Q)/P of precipitation that was evaporated and transpired ($r_S = 0.36$, $p <$

410   0.05). Thus, site-to-site variations in F_{new} were positively correlated with both potential and actual evapotranspiration. F_{new} was also inversely correlated with q_{95} ($r_S = -0.52$ at $p < 0.05$), suggesting higher F_{new} in catchments with smaller baseflow.

As new and young water fractions are strongly correlated with each other ($r_S = 0.88$, $p < 0.05$), F_{yw} exhibited similar correlations with hydroclimatic variables as those that were found for F_{new} (see Supplementary Material Figure S2S3).

415
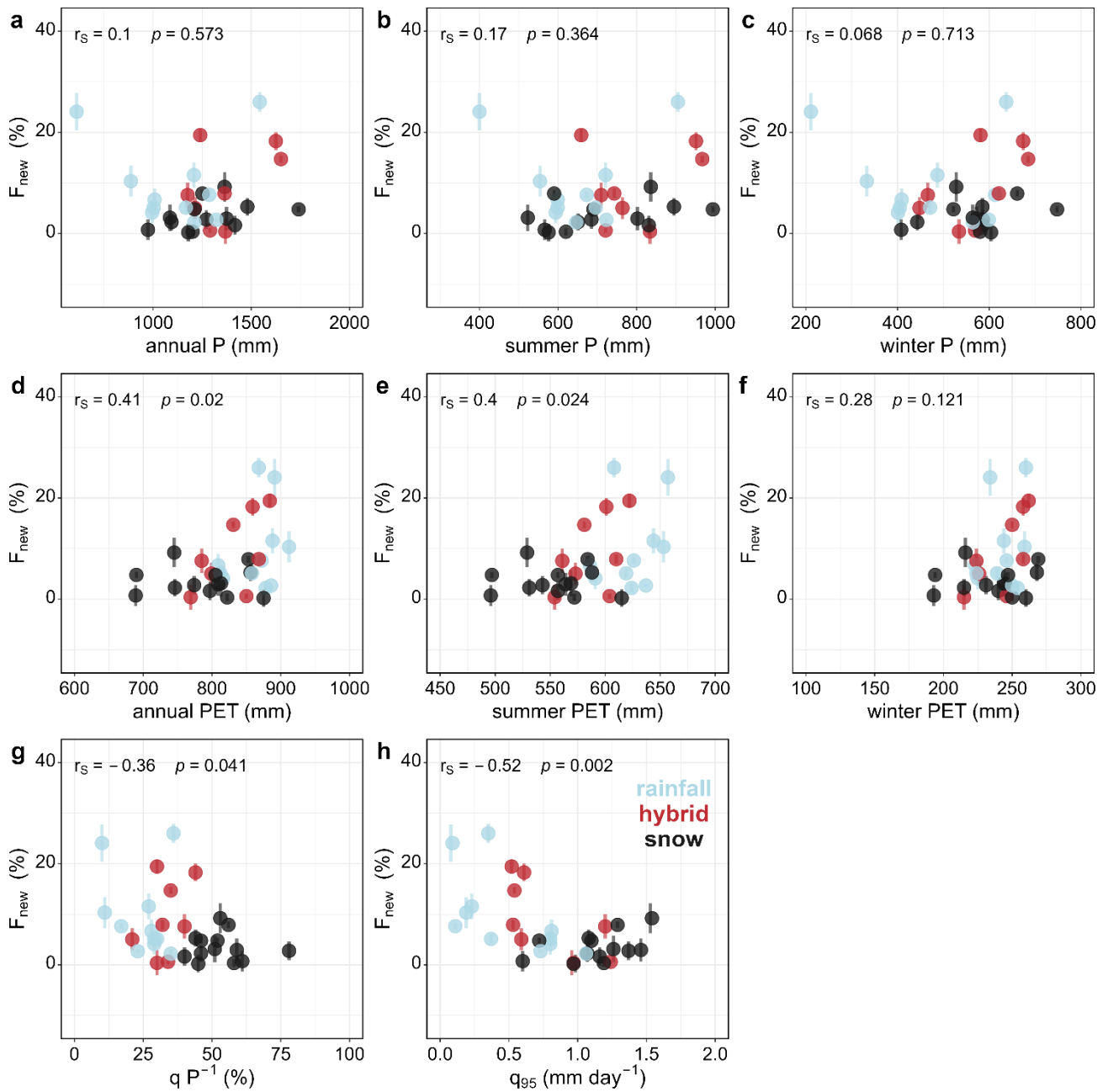
20

Figure 7: Relationships between volume-weighted new water fractions (F_{new}) and (a) annual precipitation, (b) summer (May through October) precipitation, (c) winter (November through April) precipitation, (d) annual potential evapotranspiration, (e) summer (May through October) potential evapotranspiration, (f) winter (November through April) potential evapotranspiration, (g) the fraction of annual discharge in relation to annual precipitation (q P^{-1}), and (h) q_{95}, the discharge reached or exceeded 95% of the year. The colours indicate the different precipitation

21

regimes (light blue for rainfall, red for hybrid and black for snow dominated). While F_{new} is not strongly related to precipitation, F_{new} is related to PET and the streamflow variables.

425

3.7. Relations of F_{new} to physical catchment properties

Previous studies indicate that the fractions of new (and young) water may be related to physical catchment properties. Therefore, across all 32 study catchments we compared the isotopically inferred F_{new} values with the catchment area, mean

430 catchment elevation, elevation difference, ~~the ratio of elevation difference to total catchment area,~~ as well as mean catchment slope and the fraction of slope below 10° and above 40°. To assess the effect of lithology, the fraction of (potentially karstified) carbonate sedimentary rocks and the fraction of unconsolidated debris deposits for all catchments were calculated. To assess the possible role of transpiration, the fraction of forest cover for each catchment was also calculated.

435 Figure 8 shows a systematic assessment of the relation of F_{new} and physical catchment properties. F_{new} was inversely related to catchment area, mean elevation, and elevation difference (r_S = -0.38, -0.37, and -0.59, respectively, all $p < 0.05$). Thus, F_{new} was smaller in larger catchments, higher catchments, and catchments with greater total relief. However, these three drivers are themselves strongly correlated with one another, so it is unclear which one could be considered as the primary control on F_{new}. Although the average catchment slope was not a good predictor for F_{new} (r_S = -0.20, not significant), there

440 was a much stronger correlation between F_{new} and the fraction of slope larger than 40° (r_S = -0.48, $p < 0.05$). This suggests that catchments with larger fractions of steep slopes have smaller F_{new}, but note that the fraction of slope larger 40° was also correlated to mean catchment elevation (r_S = 0.84). The fractions of potentially karstified carbonate sedimentary rocks and unconsolidated debris deposits were not related to F_{new}. Statistically significant correlations between the fraction of catchment area covered by forests and F_{new} (r_S = 0.36 at $p < 0.05$) suggest a possible role for forest vegetation in shaping

445 flowpaths and thus water ages.

Young water fractions exhibited similar relationships to catchment properties (see Supplementary Material Figure ~~S3~~S4).~~as those observed for F_{new}.~~
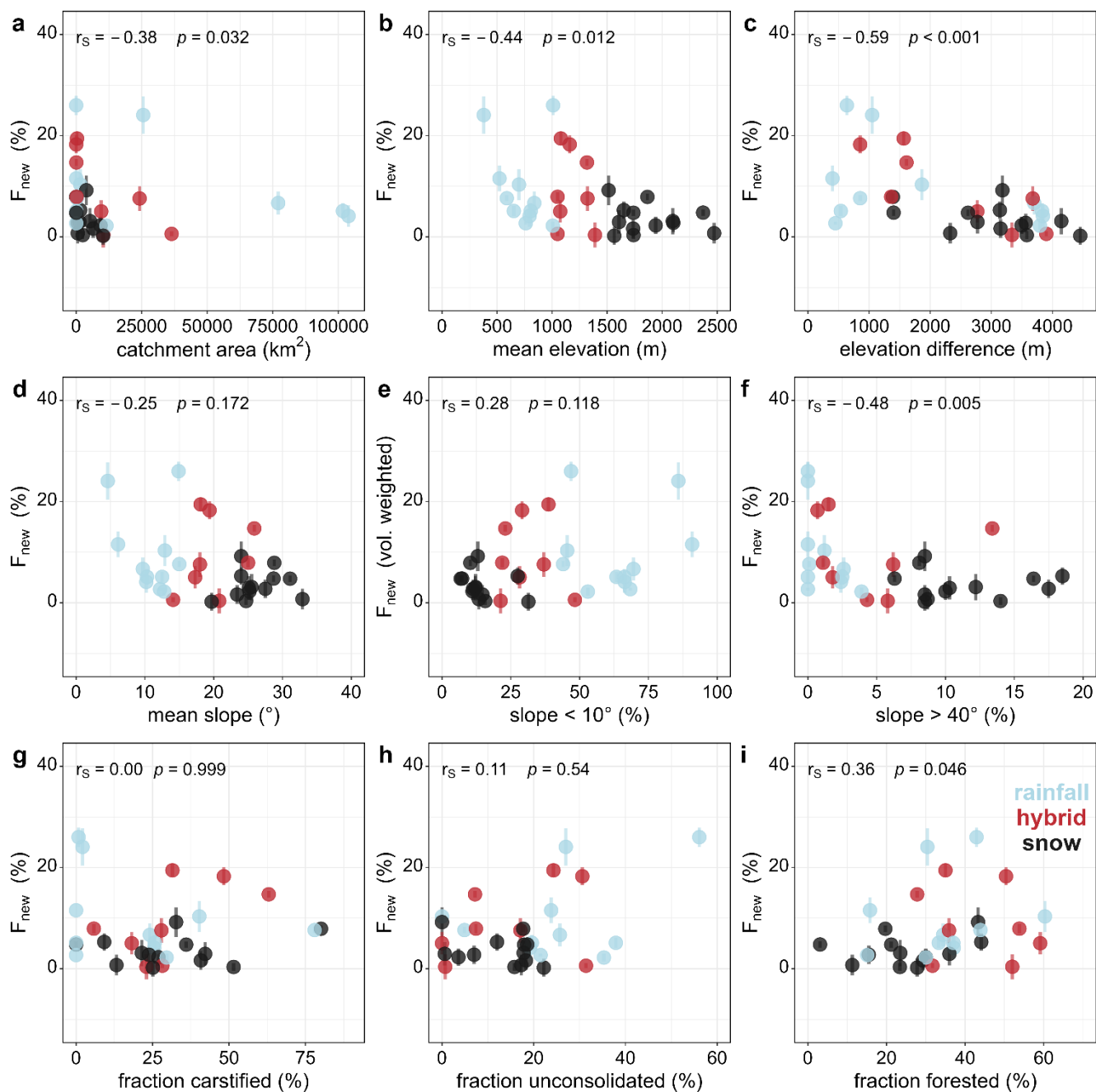
22

Figure 8: Relation of volume weighted new water fractions (F_{new}) and (a) catchment area, (b) mean elevation, (c) elevation difference, (d) mean slope, (e) fraction of slope shallower than 10°, (f) fraction of slope steeper than 40°, (g) fraction of the catchment consisting of karstified rocks, (h) fraction of the catchment covered by unconsolidated rocks, and (i) and fraction of the catchment covered by forests. The colours indicate the different precipitation

23

455 **regimes (light blue for rainfall, red for hybrid and black for snow dominated).** F_{new} **is strongly related to catchment area, elevation difference, fraction of slope steeper than 40°, and fraction of the catchment covered by forest.**

4. Discussion

460

4.1. Limitations in data availability and study design

One of the main limitations of our study (and many larger-scale isotope studies in general) is the limited availability of isotope data in streamflow and precipitation. For the presented study, we harvested all streamflow data that were available

465 for longer time periods across the European Alps, however most of these data only exist at monthly (i.e., WISA and ISOT) or 14-day (CH-IRP) resolution. While these streamflow data are sufficient to provide reasonable information on average behaviours across longer timescales (and their linkage to potential physical drivers of streamflow), it is important to remind readers that we can not infer any short-term behaviour or response to single precipitation events. For this reason, further research based on isotope data with shorter sampling intervals would enable investigations of short-term catchment drainage

470 processes (i.e., as shown in Knapp et al., 2019 or Floriancic et al., 2024).

Even more critical is the use of monthly aggregates of precipitation isotopes. Precipitation isotopologues can be very heterogeneous even within single precipitation events (e.g., Pinos et al., 2022; Allen et al., 2017). Overall, the number of stations with available precipitation isotope data is limited and single-station data collections are often not a reliable source

475 for large-basin studies that span large elevation gradients. For this reason, we calculated the monthly volume-weighed precipitation basin averages from the Piso-AI database (Nelson et al., 2021) which is to our understanding the most reliable data source for our intended application. We are well aware that other isotope interpolation methods exist (i.e., Seeger and Weiler, 2014; Allen et al., 2018), comparisons of the precipitation isotope data from Piso-AI and these methods yield similar results (see supplementary Figures S5 & S6).

480

4.1.4.2. New (F_{new}) and young (F_{yw}) water fractions across Alpine catchments

One of the main objectives of the study was to compare the physical drivers of new and young water fractions across a set of catchments of different size. Across our 32 study catchments, F_{new} and F_{yw} decreased with increasing catchment elevation

485 (Figures 3, 8b, and S4). This is consistent with previous findings of Ceperley *et al.* (2020), who observed a decrease in young water fractions above an elevation of 1500 m asl. across Swiss Alpine catchments. ~~Conversely, von Freyberg *et al.* (2018)~~Conversely, von Freyberg *et al.* (2018) found weak positive correlations with catchment elevation for a subset of our study catchments (12 of our catchments overlap with their set of 22 catchments). The relative importance of rain versus snow

24

had a clear effect on F_{new} and F_{yw}, which were ~~lower~~higher in hybrid catchments ~~than in~~and rainfall-dominated catchments,

490 and lower ~~still~~ in snow-dominated catchments (Figure 3). Conversely, Gentile *et al.*, (2023) found the highest F_{yw} in hybrid catchments, and similarly low F_{yw} in rainfall- and snow-dominated catchments. The reason for discrepancy might be that our dataset also covers much larger catchments (catchment areas in our dataset ranged from 29 km^2 to ~~103'946~~103946 km^2, versus 0.14 km^2 to 351 km^2 in Gentile *et al.* (2023).

495 F_{new} was larger in wet periods than dry periods (with means of 9.3 and 3.3 %, respectively), and larger in the summer half of the year than in the winter half of the year (means of 12.7 and 8.9 %, respectively). Similar analyses were performed on the Plynlimon dataset by Knapp *et al.* (2019), who found that wetter antecedent conditions led to higher F_{new}. At Plynlimon, F_{new} was smaller in summer (which is the drier season there), whereas in our 32 Alpine catchments, F_{new} was smaller in winter (when precipitation rates are lower, and more precipitation falls as snow). Knapp *et al.* (2019) observed strong increases in

500 7-hourly and weekly F_{new} above a precipitation threshold of roughly 5 mm day^{-1}, whereas we found that ~~only 8~~18 of 32 of our catchments showed strong increases in monthly F_{new} above a comparable precipitation threshold of roughly 175 mm month^{-1}. Readers should note that the Plynlimon subcatchments studied by Knapp *et al.* (2019) are substantially smaller (< 3.6 km^2) than ours (> 29 km^2), and the temporal resolution of their data was much higher (7h to weekly) than ours (monthly).

505 Overall, F_{new} tended to decrease downstream, from smaller headwaters to larger river basins (Section 3.5), which is consistent with the larger mean residence times that are typically estimated in larger catchments (DeWalle *et al.*, 1995; Soulsby *et al.*, 2000). Another important factor when moving from the headwaters downstream is the impact of water storage in lakes and reservoirs, as well as the potential effects of anthropogenic flow regulation. While the CH-IRP headwater catchments (Staudinger *et al.*, 2020) were carefully selected to avoid major impoundments or diversions, such complications

510 are unavoidable in the larger basins contained in our dataset. Within the Danube basin, for example, INE has several large lakes just upstream from the sampling location, and within the Rhine basin, AAT (immediately below the lake of Thun) and RHW (approximately 100 km downstream from Lake Constance) are significantly impacted by lakes. Big lakes can substantially dampen F_{new} by storing months or years of flow. Such storage yields exceptionally low F_{new} values (for example, F_{new} is 0.7, 0.4, and 0.6 % at INE, AAT, and RHW, respectively). F_{new} can also be altered by dams and their

515 accompanying reservoirs; for example, multiple large dams lie upstream of DOE, DOW, and DOH, which have F_{new} values of 6.7, 5.1, and 4.1 % (for comparison, the mean of all rainfall-dominated catchments is 9.6%).

~~4.2.~~4.3. Conceptualization of physical drivers of F_{new} and F_{yw} across the Alps
520

When looking at the effects of hydroclimatic variables and physical catchment properties on F_{new}, single-variable correlations with F_{new} should be interpreted with caution, because they may be confounded by cross-correlations between

many potential drivers (Figure **9**). For example, annual and summer *PET*, discharge fraction, q_{95}, mean slope, fraction of catchment area with slope > 40°, and fraction of catchment area with slope < 10° are all strongly related to mean catchment elevation. Thus, it remains unclear which of these variables may be a first-order control on new water fractions.
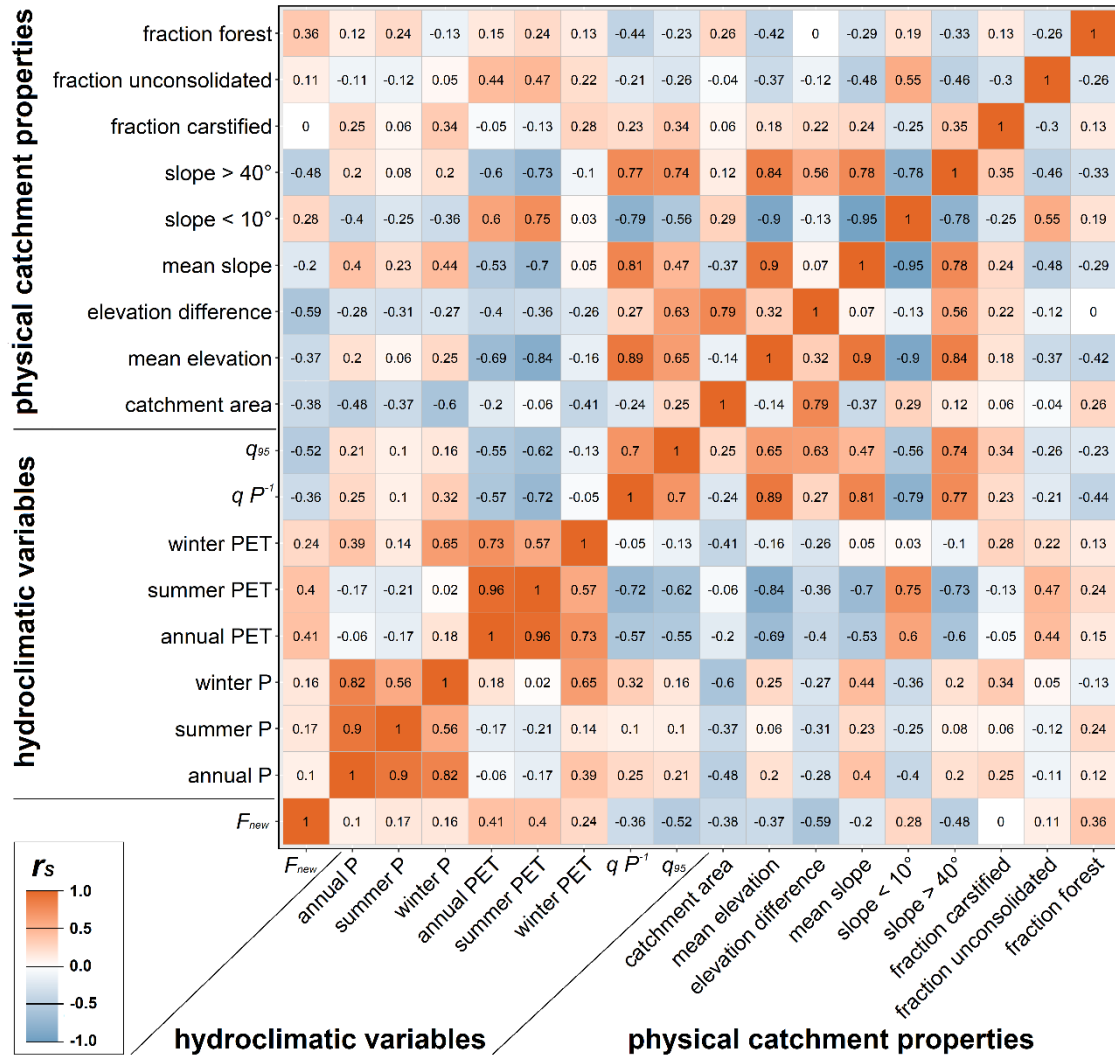

Figure 9: Spearman rank correlations between all the selected hydroclimatic variables and physical catchment characteristics across the 32 study catchments. Red colours indicate strong to intermediate positive correlations; blue colours indicate strong to intermediate inverse correlations.

Overall, we found that high fractions of new water (F_{new}) were more likely in small catchments, at low elevations, with small total relief and larger forest cover, and following months with high precipitation, whereas low F_{new} values were more likely in large catchments, at high elevations, with large total relief, and following months with low precipitation (

Figure **10**).

Von Freyberg *et al.* (2018) found significant correlations between F_{yw} and monthly precipitation. Conversely, site-to-site differences in average F_{new} and F_{yw} were only weakly correlated with precipitation (annual, summer, and winter) across our 32 sites. Nevertheless, higher precipitation in the month preceding sampling typically led to larger F_{new}, which is in line with previous findings in Knapp *et al.* (2019). Higher F_{new} values were typically found during the summer period, which receives more precipitation than the winter period (see Section 3.3).

Across the Alps, elevation is correlated with F_{new}, but also with many other variables (e.g., temperature, precipitation, *PET*, and slope) that arguably should have stronger mechanistic connections with new water fractions. Site-to-site differences in F_{new} were positively correlated with both annual *PET* and summer *PET*, and with long-term actual evapotranspiration, estimated as ET/P=(P-Q)/P (see Section 3.6). This is somewhat counterintuitive, as one might expect that if more precipitation leaves the catchment via evapotranspiration, the smaller resulting discharge flux would imply longer retention times in the catchment and thus smaller new water fractions. However, *PET* in our set of catchments is negatively correlated with elevation (Figure 9), thus it is likely that high F_{new} values in catchments with high *PET* are confounded by elevation effects rather than being solely explained by *PET*.

~~Across our 32 sites, F_{new} exhibited a strong inverse correlation with the low-flow variable q_{95} were found, suggesting higher F_{new} in catchments with smaller low flows. This is consistent with the findings of von Freyberg *et al.* (2018) showing that the quick-flow index (*QFI*) is positively correlated with F_{yw}. Although *QFI* and q_{95} are not the same, they are systematically related, as high q_{95} is more likely in catchments with low *QFI*.~~

Across our 32 sites, F_{new} exhibited a strong inverse correlation with the low-flow variable q_{95}, suggesting higher F_{new} in catchments with smaller low flows. Similarly, Gentile *et al.* (2023) found correlations between baseflow and F_{yw}. These results and ours are also consistent with the findings of von Freyberg *et al.* (2018) showing that the quick-flow index (*QFI*) is positively correlated with F_{yw}. Although *QFI* and q_{95} are not the same, they are systematically related, as high q_{95} is more likely in catchments with low *QFI*. However, also q_{95} across the European Alps is positively related with elevation (Figure 9; but see also Floriancic et al., 2022); thus large F_{new} in catchments with high q_{95} might also be affected by elevation rather than q_{95} being the sole explanation for high F_{new} values.

We observed modest (but statistically significant) negative correlations between F_{new} and catchment area, and von Freyberg *et al.* (2018) also found weak (but non-significant) correlations between catchment area and F_{yw}. However, these

relationships might be confounded by differences in the dominant precipitation regime; the correlation between F_{new} and catchment area is stronger among our hybrid catchments (Rr_S = -0.6974, $p < 0.05$) than among our rainfall-dominated or snow-dominated catchments (-0.27 and -0.39, respectively). Thus, F_{new} (and F_{yw}) appear to be inversely related to catchment area, but not so much in catchments with seasonal snow cover or glaciers (Gentile et al., 2023Gentile *et al.*, 2023; Ceperley *et al.*, 2020), which generally have small F_{new} and F_{yw} values independent of their catchment area.

We found only a weak and non-significant inverse correlation between F_{new} and mean catchment slope (r_S=-0.18), but strong inverse correlations between F_{new} and both total relief (elevation difference; r_S=-0.59) and the fraction of catchment area with slopes steeper than 40° (r_S=-0.48). These results, while not conclusive, are broadly consistent with Jasechko *et al.* (2016)'s observation of a significant negative correlation between F_{yw} and average catchment slope in their survey of 254 global rivers. Jasechko et al. (2016) argued that this decrease in young water in steep terrain may be related to subsurface storage and transport. Deep vertical infiltration is prevalent in steeper landscapes; this is also consistent with conceptual models of groundwater flow (Gleeson and Manning, 2008) showing that larger topographic gradients lead to longer subsurface flow paths. Geotechnical stresses in steep terrain also promote fracture opening and thus increase hydraulic bedrock permeability (Jasechko *et al.,* 2016; Gleeson *et al.*, 2011a), thereby facilitating deep percolation. On the other hand, catchments with steeper than 40° slopes are mainly found at higher elevations and thus tend to be snow-dominated. Here, smaller fractions of F_{new} and F_{yw} are expected due to snow storage.

High-elevation catchments tend to have smaller F_{yw} and F_{new} (e.g., Gentile *et al.*, 2023; Ceperley *et al.*, 2020 and Figure 8 in our study), and their streamflow isotopic composition may be affected by snow and glacier melt (Schmieder et al., 2016; Schmieder et al., 2018). The smaller F_{yw} and F_{new} observed at high elevations in the European Alps may result from snowpack and glacier storage leading to delayed runoff of winter precipitation. However, these high-elevation catchments also have larger elevation gradients, and thus potentially greater subsurface storage leading to longer transit times (Jasechko *et al.* 2016; Schmieder et al., 2018). A weak indication for the importance of snow processes can be found in Figure 4, where we show that F_{new} values in the summer half of the year are generally larger in most of the catchments. However, with our sample of catchments (as in several previous studies) we cannot test these hypotheses independently because catchments with large topographic gradients are also dominated by snow across the European Alps. However, this important question should be considered in further research based on a more targeted dataset that allows testing both hypotheses independently.

We found no significant correlations between F_{new} and either the fraction of area with potentially karstified carbonate sedimentary rocks or the fraction of area with unconsolidated debris deposits. This result is somewhat surprising. One would expect that karstified rocks would increase F_{new} by providing quick flow paths that allow bedrock storages to drain quickly (Hartmann et al., 2021). Furthermore, multiple previous studies have highlighted the importance of unconsolidated debris deposits in streamflow generation processes (e.g., Hood and Hayashi, 2015; Hayashi, 2019; Cochand *et al.*, 2019; Floriancic

et al., 2018)-; Gentile *et al.*, 2023;). Our analysis is based on the global GLiM database, which uses lithological classes that may be too coarse, or may be mapped at insufficient resolution, to be hydrologically informative at such rather small scales. Further analyses must await more comprehensive data on subsurface geology and near-surface geomorphological features (Gentile *et al.*, 2023; Floriancic *et al.*, 2022).

605

We also found a weak (but marginally significant) positive correlation between F_{new} and the fraction of catchment area covered by forests. ~~von~~Von Freyberg *et al.* (2018) found similar correlations with F_{yw} across Swiss headwater catchments, but Hrachowitz *et al.* (2021) found the opposite relationship for a forest removal experiment. It is somewhat surprising that the prevalence of forests is linked with higher values of F_{new}. A possible explanation might be tree roots facilitating

610   preferential pathways through macropores (Brantley *et al.*, 2017; von Freyberg *et al.*, 2018), thus increasing F_{new} and F_{yw}. However, these correlations might also be an artefact of cross-correlations with other variables, because the fraction of catchment area covered by forests is also correlated with mean elevation and fraction of catchment area with slopes steeper than 40° (R = -0.42 and -0.33, respectively). Thus, it is likely that high F_{new} in catchments with more forest cover might be affected by cross-correlations rather than forest cover being the dominant explanation for variations in F_{new}.
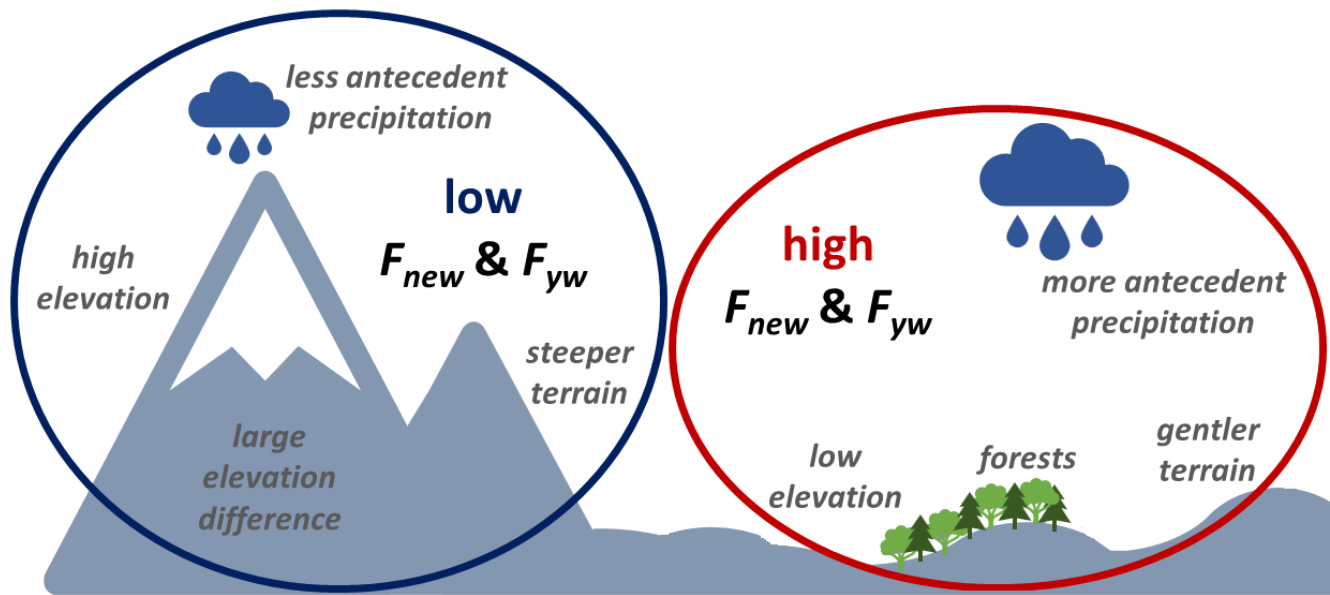
615

Figure 10: Conceptual scheme of the significant relations of hydroclimatic variables and physical catchment properties to volume weighted new water fractions (F_{new}) across the 32 Alpine catchments.

29

5. Summary and Conclusions

The Alps are an important water source for Europe, and assessing the partitioning of new (or young) waters in Alpine rivers may provide important insights for sustainable management. For this study, isotope time series from 32 catchments across the Austrian and Swiss Alps were evaluated using two recently developed methods: estimation of new water fractions (F_{new} – in this study, the fraction of water younger than about 1 month) using ensemble hydrograph separation, and estimation of young water fractions (F_{yw} – the fraction of water younger than 2-3 months) using seasonal isotope cycles. Mean F_{new} and F_{yw} decreased with mean catchment elevation and varied across precipitation regimes (Figure 3). Overall, F_{new} was higher in the summer months and higher following months with higher precipitation (Figure 4). However, strong increases in F_{new} were only observed in 8 of our 32 catchments, and only above a precipitation threshold of roughly 175 mm month^{-1}. For most catchments, F_{new} remained below 10% even when precipitation inputs were large (Figure 5). F_{new} decreased from the headwater streams to the large downstream basins of the Danube and Rhine, potentially as a result of natural dampening by larger source areas and lakes, as well as anthropogenic influences from dams and reservoirs (Figure 6). High F_{new} are more likely in small catchments, at low elevations, with small elevation gradients, in catchments with larger forest cover and when precipitation is high (Figure 4, Figure 8), whereas low F_{new} are more likely in large catchments, at high elevations, with large total relief, high baseflow (Figure 7, Figure 8), and low antecedent precipitation (Figure 4). The obtained results reveal which Alpine areas transmit recent precipitation more rapidly to runoff. However, the interpretation of the obtained results needs to be done with caution as cross-correlations exist (Figure 9) and it is not always clear to what extend the reported correlations indicate direct controls on water storage processes. The analysis also highlights the importance of further research on the effect of snow processes on partitioning of new (or young) and old waters, as well as the need for higher-resolution lithological information.

Data availability:

Daily discharge time series for 12 of the 20 Swiss sites were obtained from the CH-IRP database (Staudinger *et al.*, 2020). Discharge time series for the remaining 8 Swiss sites and for all 12 Austrian sites were obtained from the Federal Office of the Environment "Hydrological Data and forecasts" database (FOEN, 2022a) and the "Hydrographisches Jahrbuch" contained in the WISA database (Umweltbundesamt, 2022a), respectively. Daily catchment averaged precipitation was obtained from the gridded precipitation dataset E-OBS (version 20.0e) at 0.1 degree resolution (Cornes *et al.*, 2018), *PET* was calculated from the "Global Aridity Index and Potential Evapotranspiration Climate Database v2" (Trabucco and Zomer, 2019);Staudinger *et al.*, 2020). Discharge time series for the remaining 8 Swiss sites and for all 12 Austrian sites were obtained from the Federal Office of the Environment "Hydrological Data and forecasts" database (FOEN, 2022a) and the "Hydrographisches Jahrbuch" contained in the WISA database (Umweltbundesamt, 2022a), respectively. Daily catchment-averaged precipitation was obtained from the gridded precipitation dataset E-OBS (version 20.0e) at 0.1-degree resolution (Cornes *et al.*, 2018), *PET* was calculated from the "Global Aridity Index and Potential Evapotranspiration

Climate Database v2" (Trabucco and Zomer, 2019); Monthly gridded precipitation isotopes were obtained from the reanalysis database Piso.AI (Nelson *et al.*, 2021), accessible at https://isotope.bot.unibas.ch/PisoAI/. Monthly streamflow isotopes for the 12 Austrian sites were obtained from the WISA "H2O Fachdatenbank" database (Umweltbundesamt, 2022b) and for 8 Swiss stations from the NAQUA ISOT ("Nationalen Grundwasserbeobachtung – Isotopendaten") database (FOEN, 2022b). Streamflow isotopes for 12 additional stations across the Swiss Alps were obtained from the CH-IRP database (Staudinger *et al.*, 2020).

Monthly gridded precipitation isotope reanalysis database Piso.AI (Nelson *et al.*, 2021) accessible at https://isotope.bot.unibas.ch/PisoAI/ Monthly streamflow isotopes for the 12 Austrian sites were obtained from the WISA "H2O Fachdatenbank" database (Umweltbundesamt, 2022b) and for 8 Swiss stations from the NAQUA ISOT ("Nationalen Grundwasserbeobachtung – Isotopendaten") database (FOEN, 2022b). Streamflow isotopes for 12 additional stations across the Swiss Alps were obtained from the CH-IRP database (Staudinger *et al.*, 2020).

Author contribution:

MF designed the study, collected the data, ran the calculations, and wrote the first draft. All authors provided feedback during the analysis and preparation of the manuscript.

References

Allen, S. T., Keim, R. F., Barnard, H. R., McDonnell, J. J., and Renée Brooks, J.: The role of stable isotopes in understanding rainfall interception processes: a review, WIREs Water, 4, https://doi.org/10.1002/wat2.1187, 2017.

Allen, S. T., Kirchner, J. W., and Goldsmith, G. R.: Predicting Spatial Patterns in Precipitation Isotope $\delta 2H$ and $\delta 18O$ Seasonality Using Sinusoidal Isoscapes, Geophys. Res. Lett., 45, 4859–4868, https://doi.org/10.1029/2018GL077458, 2018.

Berghuijs, W. R. and Kirchner, J. W.: The relationship between contrasting ages of groundwater and streamflow: Connecting Storage and Streamflow Ages, Geophys. Res. Lett., 44, 8925–8935, https://doi.org/10.1002/2017GL074962, 2017.

Brantley, S. L., Eissenstat, D. M., Marshall, J. A., Godsey, S. E., Balogh-Brunstad, Z., Karwan, D. L., Papuga, S. A., Roering, J., Dawson, T. E., Evaristo, J., Chadwick, O., McDonnell, J. J., and Weathers, K. C.: Reviews and syntheses: on the roles trees play in building and plumbing the critical zone, Biogeosciences, 14, 5115–5142, https://doi.org/10.5194/bg-14-5115-2017, 2017.

Briffa, K. R., van der Schrier, G., and Jones, P. D.: Wet and dry summers in Europe since 1750: evidence of increasing drought: WET AND DRY SUMMERS IN EUROPE SINCE 1750, Int. J. Climatol., 29, 1894–1905, https://doi.org/10.1002/joc.1836, 2009.

690 Browne, Dr. T. J.: Derivation of a geological index for low flow studies, CATENA, 8, 265–280, https://doi.org/10.1016/0341-8162(81)90010-2, 1981.

Ceperley, N., Zuecco, G., Beria, H., Carturan, L., Michelon, A., Penna, D., Larsen, J., and Schaefli, B.: Seasonal snow cover decreases young water fractions in high Alpine catchments, Hydrological Processes, 34, 4794–4813, https://doi.org/10.1002/hyp.13937, 2020.

Cochand, M., Christe, P., Ornstein, P., and Hunkeler, D.: Groundwater Storage in High Alpine Catchments and its
695 Contribution to Streamflow, Water Resources Research, 55, 2613–2630, 2019.

Cornes, R. C., van der Schrier, G., van den Besselaar, E. J. M., and Jones, P. D.: An Ensemble Version of the E-OBS Temperature and Precipitation Data Sets, J. Geophys. Res. Atmos., 123, 9391–9409, https://doi.org/10.1029/2017JD028200, 2018.

Craig, H. and Gordon, L. I.: Deuterium and Oxygen 18 Variations in the Ocean and the Marine Atmosphere, 1965.

700 DeWalle, D. R., Edwards, P. J., Swistock, B. R., Drimmie, R. J., and Aravena, R.: Seasonal isotope hydrology of Appalachian forest catchments, In: Gottschalk, Kurt W.; Fosbroke, Sandra L. C., ed. Proceedings, 10th Central Hardwood Forest Conference; 1995 March 5-8; Morgantown, WV.: Gen. Tech. Rep. NE-197. Radnor, PA: U.S. Department of Agriculture, Forest Service, Northeastern Forest Experiment Station. p.296, 197, 1995.

Fleckenstein, J. H., Niswonger, R. G., and Fogg, G. E.: River-Aquifer Interactions, Geologic Heterogeneity, and Low-Flow
705 Management, Ground Water, 44, 837–852, https://doi.org/10.1111/j.1745-6584.2006.00190.x, 2006.

Floriancic, M. G., Meerveld, I., Smoorenburg, M., Margreth, M., Naef, F., Kirchner, J. W., and Molnar, P.: Spatio-temporal variability in contributions to low flows in the high Alpine Poschiavino catchment, Hydrological Processes, 32, 3938–3953, https://doi.org/10.1002/hyp.13302, 2018.

Floriancic, M. G., Spies, D., van Meerveld, I. H. J., and Molnar, P.: A multi-scale study of the dominant catchment
710 characteristics impacting low-flow metrics, Hydrological Processes, 36, https://doi.org/10.1002/hyp.14462, 2022.

Floriancic, M. G., Allen, S. T., and Kirchner, J. W.: Young and new water fractions in soil and hillslope waters, EGUsphere, 1–24, https://doi.org/10.5194/egusphere-2024-437, 2024.

FOEN; Hydrological Data and forecasts: https://www.hydrodaten.admin.ch/en/stations-and-data.html, last access: 5 December 2022.

715 FOEN; NAQUA ISOT: https://www.bafu.admin.ch/bafu/en/home/topics/water/info-specialists/state-of-waterbodies/state-of-groundwater/naqua-national-groundwater-monitoring/isot-module.html, last access: 5 December 2022.

von Freyberg, J., Studer, B., and Kirchner, J. W.: A lab in the field: high-frequency analysis of water quality and stable isotopes in stream water and precipitation, Hydrol. Earth Syst. Sci., 21, 1721–1739, https://doi.org/10.5194/hess-21-1721-2017, 2017.

von Freyberg, J., Allen, S. T., Seeger, S., Weiler, M., and Kirchner, J. W.: Sensitivity of young water fractions to hydro-climatic forcing and landscape properties across 22 Swiss catchments, Hydrology and Earth System Sciences, 22, 3841–3861, https://doi.org/10.5194/hess-22-3841-2018, 2018.

Gentile, A., Canone, D., Ceperley, N., Gisolo, D., Previati, M., Zuecco, G., Schaefli, B., and Ferraris, S.: Towards a conceptualization of the hydrological processes behind changes of young water fraction with elevation: a focus on mountainous alpine catchments, Hydrology and Earth System Sciences, 27, 2301–2323, https://doi.org/10.5194/hess-27-2301-2023, 2023.

Gleeson, T. and Manning, A. H.: Regional groundwater flow in mountainous terrain: Three-dimensional simulations of topographic and hydrogeologic controls: Regional groundwater flow, Water Resour. Res., 44, https://doi.org/10.1029/2008WR006848, 2008.

Gleeson, T., Marklund, L., Smith, L., and Manning, A. H.: Classifying the water table at regional to continental scales: WATER TABLE AT CONTINENTAL SCALES, Geophys. Res. Lett., 38, n/a-n/a, https://doi.org/10.1029/2010GL046427, 2011a.

Gleeson, T., Smith, L., Moosdorf, N., Hartmann, J., Dürr, H. H., Manning, A. H., van Beek, L. P. H., and Jellinek, A. M.: Mapping permeability over the surface of the Earth: MAPPING GLOBAL PERMEABILITY, Geophys. Res. Lett., 38, n/a-n/a, https://doi.org/10.1029/2010GL045565, 2011b.

Gleeson, T., Befus, K. M., Jasechko, S., Luijendijk, E., and Cardenas, M. B.: The global volume and distribution of modern groundwater, Nature Geosci, 9, 161–167, https://doi.org/10.1038/ngeo2590, 2016.

Hartmann, A., Jasechko, S., Gleeson, T., Wada, Y., Andreo, B., Barberá, J. A., Brielmann, H., Bouchaou, L., Charlier, J.-B., Darling, W. G., Filippini, M., Garvelmann, J., Goldscheider, N., Kralik, M., Kunstmann, H., Ladouche, B., Lange, J., Lucianetti, G., Martín, J. F., Mudarra, M., Sánchez, D., Stumpp, C., Zagana, E., and Wagener, T.: Risk of groundwater contamination widely underestimated because of fast flow into aquifers, Proc. Natl. Acad. Sci. U.S.A., 118, e2024492118, https://doi.org/10.1073/pnas.2024492118, 2021.

Hartmann, J. and Moosdorf, N.: The new global lithological map database GLiM: A representation of rock properties at the Earth surface, Geochemistry, Geophysics, Geosystems, 13, https://doi.org/10.1029/2012GC004370, 2012.

Hayashi, M.: Alpine Hydrogeology: The Critical Role of Groundwater in Sourcing the Headwaters of the World, Groundwater, gwat.12965, https://doi.org/10.1111/gwat.12965, 2019.

Hood, J. L. and Hayashi, M.: Characterization of snowmelt flux and groundwater storage in an alpine headwater basin, Journal of Hydrology, 521, 482–497, https://doi.org/10.1016/j.jhydrol.2014.12.041, 2015.

Hrachowitz, M., Soulsby, C., Tetzlaff, D., Dawson, J. J. C., and Malcolm, I. A.: Regionalization of transit time estimates in montane catchments by integrating landscape controls, Water Resources Research, 45, https://doi.org/10.1029/2008WR007496, 2009.

Hrachowitz, M., Stockinger, M., Coenders-Gerrits, M., van der Ent, R., Bogena, H., Lücke, A., and Stumpp, C.: Reduction of vegetation-accessible water storage capacity after deforestation affects catchment travel time distributions and increases young water fractions in a headwater catchment, Hydrol. Earth Syst. Sci., 25, 4887–4915, https://doi.org/10.5194/hess-25-4887-2021, 2021.

Water Resources Programme IAEA; Global Network of Isotopes in Precipitation: http (GNIP): https://www-naweb.iaea.org/napc/ih/IHS_resources services/networks/gnip.html, last access: 11 July 201925 October 2022.

Water Resources Programme -IAEA; Global Network of Isotopes in Rivers: (GNIR): http://www-naweb.iaea.org/napc/ih/IHS_resources_gnir.html, last access: 11 July 201925 October 2022.

760   Jasechko, S., Kirchner, J. W., Welker, J. M., and McDonnell, J. J.: Substantial proportion of global streamflow less than three months old, Nature Geoscience, 9, 126, 2016.

Jasechko, S., Perrone, D., Befus, K. M., Bayani Cardenas, M., Ferguson, G., Gleeson, T., Luijendijk, E., McDonnell, J. J., Taylor, R. G., Wada, Y., and Kirchner, J. W.: Global aquifers dominated by fossil groundwaters but wells vulnerable to modern contamination, Nature Geosci, 10, 425–429, https://doi.org/10.1038/ngeo2943, 2017.

765   Kirchner, J. W.: A double paradox in catchment hydrology and geochemistry, Hydrological Processes, 17, 871–874, https://doi.org/10.1002/hyp.5108, 2003.

Kirchner, J. W.: Aggregation in environmental systems – Part 1: Seasonal tracer cycles quantify young water fractions, but not mean transit times, in spatially heterogeneous catchments, Hydrol. Earth Syst. Sci., 20, 279–297, https://doi.org/10.5194/hess-20-279-2016, 2016a.

770   Kirchner, J. W.: Aggregation in environmental systems – Part 2: Catchment mean transit times and young water fractions under hydrologic nonstationarity, Hydrol. Earth Syst. Sci., 20, 299–328, https://doi.org/10.5194/hess-20-299-2016, 2016b.

Kirchner, J. W.: Quantifying new water fractions and transit time distributions using ensemble hydrograph separation: theory and benchmark tests, Hydrology and Earth System Sciences, 23, 303–349, https://doi.org/10.5194/hess-23-303-2019, 2019.

Kirchner, J. W. and Knapp, J. L. A.: Ensemble hydrograph separation scripts - EnviDat, 2020a.

775   Kirchner, J. W. and Knapp, J. L. A.: Technical note: Calculation scripts for ensemble hydrograph separation, Hydrol. Earth Syst. Sci., 24, 5539–5558, https://doi.org/10.5194/hess-24-5539-2020, 2020b.

Kirchner, J. W., Benettin, P., and Meerveld, I. van: Instructive Surprises in the Hydrological Functioning of Landscapes:., https://doi.org/10.1146/annurev-earth-071822-100356, https://doi.org/10.1146/annurev-earth-071822-100356, 2023.

Klaus, J. and McDonnell, J. J.: Hydrograph separation using stable isotopes: Review and evaluation, Journal of Hydrology,
780   505, 47–64, https://doi.org/10.1016/j.jhydrol.2013.09.006, 2013.

Knapp, J. L. A., Neal, C., Schlumpf, A., Neal, M., and Kirchner, J. W.: New water fractions and transit time distributions at Plynlimon, Wales, estimated from stable water isotopes in precipitation and streamflow, Hydrology and Earth System Sciences, 23, 4367–4388, https://doi.org/10.5194/hess-23-4367-2019, 2019.

Mastrotheodoros, T., Pappas, C., Molnar, P., Burlando, P., Manoli, G., Parajka, J., Rigon, R., Szeles, B., Bottazzi, M.,
785   Hadjidoukas, P., and Fatichi, S.: More green and less blue water in the Alps during warmer summers, Nat. Clim. Chang., 10, 155–161, https://doi.org/10.1038/s41558-019-0676-5, 2020.

McDonnell, J. J. and Beven, K.: Debates—The future of hydrological sciences: A (common) path forward? A call to action aimed at understanding velocities, celerities and residence time distributions of the headwater hydrograph, Water Resources Research, 50, 5342–5350, https://doi.org/10.1002/2013WR015141, 2014.

790   McDonnell, J. J., McGuire, K., Aggarwal, P., Beven, K. J., Biondi, D., Destouni, G., Dunn, S., James, A., Kirchner, J., Kraft, P., Lyon, S., Maloszewski, P., Newman, B., Pfister, L., Rinaldo, A., Rodhe, A., Sayama, T., Seibert, J., Solomon, K., Soulsby, C., Stewart, M., Tetzlaff, D., Tobin, C., Troch, P., Weiler, M., Western, A., Wörman, A., and Wrede, S.: How old

is streamwater? Open questions in catchment transit time conceptualization, modelling and analysis, Hydrological Processes, 24, 1745–1754, https://doi.org/10.1002/hyp.7796, 2010.

795 Neal, C. and Rosier, P. T. W.: Chemical studies of chloride and stable oxygen isotopes in two conifer afforested and moorland sites in the British uplands, Journal of Hydrology, 115, 269–283, https://doi.org/10.1016/0022-1694(90)90209-G, 1990.

Nelson, D. B., Basler, D., and Kahmen, A.: Precipitation isotope time series predictions from machine learning applied in Europe, Proceedings of the National Academy of Sciences, 118, e2024107118, https://doi.org/10.1073/pnas.2024107118, 800 2021.

Pinos, J., Llorens, P., and Latron, J.: High-resolution temporal dynamics of intra-storm isotopic composition of stemflow and throughfall in a Mediterranean Scots pine forest, Hydrological Processes, 36, e14641, https://doi.org/10.1002/hyp.14641, 2022.

Schmieder, J., Hanzer, F., Marke, T., Garvelmann, J., Warscher, M., Kunstmann, H., and Strasser, U.: The importance of 805 snowmelt spatiotemporal variability for isotope-based hydrograph separation in a high-elevation catchment, Hydrology and Earth System Sciences, 20, 5015–5033, https://doi.org/10.5194/hess-20-5015-2016, 2016.

Schmieder, J., Garvelmann, J., Marke, T., and Strasser, U.: Spatio-temporal tracer variability in the glacier melt end-member — How does it affect hydrograph separation results?, Hydrological Processes, 32, 1828–1843, https://doi.org/10.1002/hyp.11628, 2018.

810 Schürch, M., Kozel, R., Schotterer, U., and Tripet, J.-P.: Observation of isotopes in the water cycle—the Swiss National Network (NISOT), Environmental Geology, 45, 1–11, https://doi.org/10.1007/s00254-003-0843-9, 2003.

Seeger, S. and Weiler, M.: Reevaluation of transit time distributions, mean transit times and their relation to catchment topography, Hydrol. Earth Syst. Sci., 18, 4751–4771, https://doi.org/10.5194/hess-18-4751-2014, 2014.

Segura, C., James, A. L., Lazzati, D., and Roulet, N. T.: Scaling relationships for event water contributions and transit times 815 in small-forested catchments in Eastern Quebec, Water Resources Research, 48, https://doi.org/10.1029/2012WR011890, 2012.

Sklash, M. G. and Farvolden, R. N.: The role of groundwater in storm runoff, Journal of Hydrology, 43, 45–65, https://doi.org/10.1016/0022-1694(79)90164-1, 1979.

Soulsby, C., Malcolm, R., Helliwell, R., Ferrier, R. C., and Jenkins, A.: Isotope hydrology of the Allt a' Mharcaidh 820 catchment, Cairngorms, Scotland: implications for hydrological pathways and residence times, Hydrol. Process., 14, 747–762, https://doi.org/10.1002/(SICI)1099-1085(200003)14:4<747::AID-HYP970>3.0.CO;2-0, 2000.

Staudinger, M., Seeger, S., Herbstritt, B., Stoelzle, M., Seibert, J., Stahl, K., and Weiler, M.: The CH-IRP data set: a decade of fortnightly data on δ2H and δ18O in streamflow and precipitation in Switzerland, Earth Syst. Sci. Data, 12, 3057–3066, https://doi.org/10.5194/essd-12-3057-2020, 2020.

825 Stockinger, M. P., Bogena, H. R., Lücke, A., Stumpp, C., and Vereecken, H.: Time variability and uncertainty in the fraction of young water in a small headwater catchment, Hydrology and Earth System Sciences, 23, 4333–4347, https://doi.org/10.5194/hess-23-4333-2019, 2019.

Trabucco, A. and Zomer, R.: Global Aridity Index and Potential Evapotranspiration (ET0) Climate Database v2, https://doi.org/10.6084/m9.figshare.7504448.v3, 2019.

830   Umweltbundesamt; Hydrographisches Jahrbuch - WISA: https://wasser.umweltbundesamt.at/hydjb/, last access: 5 December 2022.

Umweltbundesamt; WISA H2O Fachdatenbank: https://wasser.umweltbundesamt.at/h2odb/, last access: 5 December 2022.

Weingartner, R., Viviroli, D., and Schädler, B.: Water resources in mountain regions: a methodological approach to assess the water balance in a highland-lowland-system, Hydrol. Process., 21, 578–585, https://doi.org/10.1002/hyp.6268, 2007.

835